JAERI-Research
98-038

ACTINIDE LEVEL DENSITY PARAMETER SYSTEMATICS

August 1998

V. M. MASLOV* and Yu. V. PORODZINSKIJ*

日本原子力研究所
Japan Atomic Energy Research Institute

編集兼発行　　日本原子力研究所

JAERI-Research 98-038

Actinide Level Density Parameter Systematics

V. M. MASLOV*※ and Yu. V. PORODZINSKIJ*

Department of Nuclear Energy System
Tokai Research Establishment
Japan Atomic Energy Research Institute
Tokai-mura, Naka-gun, Ibaraki-ken

(Received July 3, 1998)

Neutron resonance spacing data for actinides (Th-Cf) are analyzed to obtain level density parameters. Cumulative plots of low-lying levels are fitted with a constant temperature model. Systematic trends of constant temperature model parameters U_c,U_o, T are revealed.

Keywords: Actinide, Level Density, Systematics, Resonance Spacing

※ Visiting Researcher

* Radiation Physics and Chemistry Problems Institute, Minsk, Belarus

JAERI-Research 98-038

アクチニド準位密度パラメータの系統性

日本原子力研究所東海研究所エネルギーシステム研究部
V. M. MASLOV*※・Yu. V. PORODZINSKIJ*

（1998年7月3日受理）

アクチニド核種の中性子共鳴間隔のデータを解析し、ThからCfまでの準位密度パラメータを求めた。低励起準位の累積プロットを定温度模型でフィットした。定温度模型パラメータUc、Uo、Tの系統性が得られた。

東海研究所　〒319－1195　茨城県那珂郡東海村白方白根2－4
※　外国人研究者招聘制度による招聘研究員
*　放射線物理・化学問題研究所、ミンスク、ベラルーシ共和国

Contents

目　　次

1 Introduction

Level density is one of the main ingredients of statistical model calculations. Level density of relevant compound, residual and fissioning nuclei define transmission coefficients of radiative decay, neutron scattering and fission channels. Evaluated values of average reduced neutron widths and level spacings in resolved resonance region are usually used for fixing optical and statistical model parameters. Rather sophisticated methods are used as an alternative to averaging of experimental resolved resonance parameter values. However, such methods which take into account resonance missing may give rather discrepant results. Main drawback of these methods is due to consideration of the level missing due to poor energy resolution and discrimination threshold separately, while both factors seem to be correlated [1]. In other words, two strong resonances are usually resolved even being closely spaced, while a weak resonance, if shadowed by the strong one, always remains unresolved. Actually actinide neutron resonance spacing data are available only for 32 nuclei from Th up to Cf, so it is highly desirable to obtain extra knowledge on level density of other actinide nuclei based on this rather scarce data base.

2 Neutron Resonance Spacing Estimation

The present method of average resonance parameter evaluation is described in detail elsewhere [2]. Below are given the main points of the model. In case of even target nuclei we deal with one system of $s-$wave resonances with spin values of 1/2, the well known Porter-Thomas [3] formula for reduced neutron width distribution and the Wigner [4] formula for level spacing distribution are valid. In case of odd and odd-odd target nuclei we deal with two systems of $s-$wave resonances with spin values of $I \pm 1/2$, I being the target nucleus spin. Resonance level spacing distributions involved in our approach for even and odd nuclei differ considerably (see Fig.1). Level spacing distribution as well as neutron reduced width distribution assume possible coexistence of two systems of resonances with different spins. Resonances with the same spin are repulsed, which means that small resonance spacing are of low probability. In case of odd nuclei the spins of closely spaced levels might be different and the influence of level repulsion is diminished. This results in much greater resonance missing for odd target nuclei, as compared with even ones. The probability to resolve neutron resonances in the experiment $Y(x, y, E)$ was modelled as

$$Y(x,y,E) = \frac{(1+a)}{\left[a + exp\left(\frac{c\Delta(E)}{(x^s y<D>)}\right)\right]\left[\left(\frac{x_o}{x}\right)^p + 1\right]} \tag{1}$$

where $\Delta(E)$ - is experimental energy resolution; x_o - is diffusive threshold of resonance width discrimination; $p-$ defines the curvature of the discrimination threshold; s - defines correlation between resonance missing due to it's weakness and poor resolution; c - parameter, which determines rate of the level missing when the energy resolution diminishes; a - is normalization constant; $x = g\Gamma_n^o/\langle g\Gamma_n^o\rangle$, $y = D/\langle D\rangle$, Γ_n^o is reduced neutron width, D is neutron resonance spacing, $g = \frac{(2J+1)}{2(2I+1)}$, J and I are compound and target nucleus spin values, respectively. Function $Y(x,y,E)$ has the following asymptotic behavior: it decreases to zero when x, y, $x^s y$, $1/x_o$ or $\langle D\rangle/\Delta(E)$ go to zero, and becomes unity when x, y, $x^s y$, $1/x_o$ or $\langle D\rangle/\Delta(E)$ increase.

Average resonance and resolution function parameters are defined by fitting experimental neutron widths and level spacings distributions with theoretically expected distributions using maximum likelihood method. Evaluated values of average level spacings and $s-$wave strength functions are compared with other evaluations in Table 1, where note that compound nuclei mass numbers are indicated. Resonance parameters in this evaluation were taken from BNL-325, except those marked with asterisk, which had been taken from original evaluations [5, 6]. We claim greater reliability of our results, since we fit both reduced neutron widths and level spacings distributions. For example, in case of thoroughly investigated ^{238}U target nuclide various estimates almost coincide, while in less favorable cases the discrepancies might appear. For example, neutron resonance spacing $\langle D\rangle = 2.973$ eV for ^{237}U target nuclide was obtained, which is much lower than other estimates, although it is still compatible with them within attributed error estimates. Figures 2 and 3 show the cumulative sum of resolved resonance levels for ^{238}U and ^{237}U target nuclides as dependent on the neutron energy E_n. Solid line shows estimated number of resonances for spacing values $\langle D\rangle$, obtained by fitting resonance spacing distribution. Dashed lines above and below the solid line demonstrate the dependence of the estimated number of resonances on the statistical error of neutron resonance spacing $\langle D\rangle$. Statistical error of the neutron resonance spacing $\langle D\rangle$ depends on the number of resonances N roughly as $\sim 1/\sqrt{N}$ [4]. The missing of levels is evident at much lower energies in case of ^{237}U, than in case of ^{238}U target nuclide. Figures 4 and 5 show the comparison of expected and observed distributions for neutron resonance spacings. The expected distributions shown on Figs. 4, 5 demonstrate the effect of resonance missing. We used also quantile representation of expected resonance distribution, which is shown in Figs. 4 and 5 as solid line histogram. Intervals for $D/\langle D\rangle$ values divide the whole range of $y = D/\langle D\rangle$ so that areas under expected distribution over each interval are equal. Typical number of intervals is from 5 to 10, it depends on the number of observed resonances. There is evidence that the expected distributions are consistent with the experimental data within statistical errors. That is the reason to consider the estimates of average spacing $\langle D \rangle$ reliable. With the proposed method we may treat experimental data sets with up to ~50% levels missing.

Table 1 Average level spacings and neutron strength functions of s−wave resonances

Nuclide	$\langle D \rangle$, eV [9]	$\langle D \rangle$, eV [10]	$\langle D \rangle$, eV	$S_o \times 10^4$ [9]	$S_o \times 10^4$
^{230}Th	.53±.15	.62±.12	.455±.069	.62±.16	1.388±0.687
^{231}Th	9.6±1.3	9.6±1.5	12.386±1.338	1.5±0.4	1.472±0.455
^{233}Th	16.8±1.0	16.6±0.6	17.380±0.600	.84±.07	.800±.080
^{232}Pa	.45±.05	.45±.05	.444±.059	.81±.10	.775±.353
^{234}Pa	.59±.09	.70±.10	.503±.095	.75±.06	.802±.411
^{233}U	4.6±0.7	4.6±0.7	4.717±0.381	.91±.20	.881±.296
^{234}U	.55±.05	.55±.05	0.508±0.025	1.04±0.07	1.073±0.144
^{235}U	10.6±0.5	12.0±0.8	11.488±0.551	.86±.11	.809±.112
^{236}U	.44±.06	.43±.01	.488±.018	1.0±0.1	1.013±0.104
^{237}U	14.7±0.8	15±1 16	15.261±0.687	1.0±0.1	1.028±0.130
^{238}U	3.5±0.8	3.5±0.8	2.973±0.386		
^{239}U	20.9±1.1	20.8±0.3	20.761±0.799	1.2±0.1	1.169±0.130
^{238}Np	.52±.04	.57±.03	.553±.022	1.02±0.06	.954±.075
^{239}Pu	9.0±0.7	8±1	8.301±0.598	1.3±0.3	1.285±0.269
^{240}Pu	2.3±0.1	2.20±0.05	2.308±0.076	1.3±0.1	1.302±0.126
^{241}Pu	13.6±0.7	12.4±0.7	13.440±0.720	.93±.08	1.065±0.164
^{242}Pu	.9±.1	.73±.08	1.070±0.056	1.06±0.14	1.073±0.162
^{243}Pu	15.5±1.7	13.5±1.5	13.526±0.812	.9±.1	.912±.154
^{245}Pu	17±3		18.992±2.868	.9±.3	1.243±0.522
^{242}Am*	.55±.05	.58±.04	.551±.034	.90±.09	.896±.115
^{243m}Am*	.40±.08	.40±.08	.271±.024	1.4±0.3	1.215±0.247
^{244}Am *	.60±.06	.73±.06	.621±.042	.98±.09	.900±.131
^{243}Cm	25±8	14±3	10.082±1.976	.9±.3	.763±.395
^{244}Cm*	1.1±0.2	.75±.15	.809±.078	1.30±0.26	1.050±0.230
^{245}Cm	12±1	11.8±1.2	11.571±1.041	.92±.17	1.061±0.272
^{246}Cm*	1.4±0.1	1.3±0.2	1.006±0.056	1.18±0.27	1.151±0.185
^{247}Cm*	34±7	30±5	17.58±4.0	.50±.16	.91±.34
^{248}Cm	1.4±0.1	1.8±0.3	1.181±0.164	.75±.18	.935±.278
^{249}Cm	33±5	28±5	38.478±3.578	1.0±0.2	1.013±0.238
^{250}Bk	1.0±0.1	1.0±0.1	1.195±0.136	.90±.20	1.095±0.300
^{250}Cf	.7±.1	.7±.1	1.094±0.078	1.00±0.17	1.031±0.199
^{253}Cf	27±3	27±4	26.747±2.407		

2.1 Level Density

Neutron resonance spacing data for Th - Cf nuclei exhibit grouping for even target nuclei and for odd and odd-odd targets (see Fig. 6). Neutron resonance spacings from fourth column of Table 1 will be used for definition of level density model parameters. Neutron resonance spacings were calculated with a phenomenological model by Ignatyuk et al. [7], which takes into account shell, pairing and collective effects in a consistent way:

$$\rho(U,J,\pi) = K_{rot}(U,J)K_{vib}(U)\rho_{qp}(U,J,\pi), \tag{2}$$

where $\rho_{qp}(U,J,\pi)$ is the quasiparticle level density, $K_{rot}(U,J)$ and $K_{vib}(U)$ are factors of rotational and vibrational enhancement of the level density. The relation (2) holds in an adiabatic approximation, when collective and intrinsic excitation contributions to the total level density $\rho(U,J,\pi)$ are factorized. The quasiparticle level density $\rho_{qp}(U,J,\pi)$ is defined as follows

$$\rho_{qp}(U,J,\pi) = \frac{(2J+1)\omega_{qp}(U)}{4\sqrt{2\pi}\sigma_\perp^2\sigma_\parallel}\exp\left(-\frac{J(J+1)}{2\sigma_\perp^2}\right). \tag{3}$$

Intrinsic state density $\omega_{qp}(U)$ is defined as

$$\omega_{qp}(U) = \frac{\exp(S)}{(2\pi)^{3/2}D^{1/2}}, \tag{4}$$

where S is the entropy and D is the determinant, composed of the second order partial derivatives of the statistical sum [7]. Spin distribution parameter is given by $\sigma_\parallel^2 = F_\parallel\, t$, where t is thermodynamic temperature. The momentum of inertia $F_\parallel$ is defined as

$$F_\parallel = 6/\pi^2 < m^2 > (1 - 2/3\varepsilon), \tag{5}$$

where $\langle m^2\rangle = 0.24A^{2/3}$ is the average value of the squared projection of the angular momentum of the single-particle states on the symmetry axis and ε is quadrupole deformation parameter. The shell correction dependence of the main level density $a-$parameter is defined using the following equation [7]:

$$a(U) = \begin{cases} \tilde{a}(1+\ \delta W f(U-E_{cond})/(U-E_{cond})), & U > U_{cr} = 0.47a_{cr}\Delta^2\ -n\Delta \\ a(U_{cr}) = a_{cr} & U \le U_{cr}\ = 0.47a_{cr}\Delta^2\ -n\Delta, \end{cases} \tag{6}$$

where $n = 0,\ 1,\ 2$ denotes even-even, odd-A and odd-odd nuclei, respectively; $f(x) = 1 - exp(-\gamma x)$, is the dimensionless function, defining the shell effects dumping; the condensation energy is defined as $E_{cond} = 0.152a_{cr}\Delta^2 - n\Delta$, with the correlation function Δ; $\tilde{a}$ is the asymptotic a-parameter value at high excitation energies, while a_{cr} is $a-$parameter value at critical excitation energy U_{cr}. At excitations $U \ge U_{cr}$, the equation of state is written as $U = at^2 + E_{cond}$. The main parameter of the level density a was obtained by fitting the neutron resonance spacing $\langle D \rangle$.

The collective contribution of the level density of deformed nuclei is defined by the nuclear deformation order of symmetry. The actinide nuclei at equilibrium deformation are axially symmetric. For a deformed axially symmetric nucleus, the factor of rotational enhancement is expressed as

$$K_{rot}(U) = \sum_{K=-J}^{K=J} \exp\left(\frac{-K^2}{K_o^2}\right) \simeq \sigma_\perp^2 = F_\perp t, \tag{7}$$

$$K_o^2 = \frac{\sigma_\parallel^2 \sigma_\perp^2}{\sigma_\perp^2 - \sigma_\parallel^2}, \tag{8}$$

where $\sigma_\perp^2$ is the spin cutoff parameter, $F_\perp$ is the nuclear momentum of inertia (perpendicular to the symmetry axis), which equals the rigid-body value at high excitation energies, where the pairing correlations are destroyed,

$$F_\perp = 0.4 m_o r_o^2 A^{5/3}(1 + 1/3\varepsilon), \tag{9}$$

with m_o as the nucleon mass and $r_o = 1.24$ fm, and takes an experimental value F_o at zero temperature and is interpolated in between, using the pairing model . Factor of vibrational level density enhancement [7] $K_{vib}(U)$ is defined as

$$K_{vib}(U) = \exp\left[1.7\left(\frac{3 m_o A}{4\pi\sigma_{LD}}\right)^{2/3} t^{4/3}\right], \tag{10}$$

where σ_{LD} denotes the surface tension coefficient in a liquid drop model, normalized as $4\pi r_o^2 \sigma_{LD} = 18$ MeV. The closed-form expressions for thermodynamic temperature and other relevant equations which one needs to calculate $\rho(U, J, \pi)$ are provided by Ignatyuk et al. [7]

The parameters of the level density model for equilibrium deformations are: shell correction δW, pairing correlation function Δ at equilibrium deformations, quadrupole deformation ε and momentum of inertia at zero temperature $F_o/\hbar^2$. For ground state deformations the shell corrections were calculated as $\delta W = M^{exp} - M^{MS}$, where M^{MS} denotes liquid drop mass (LDM), calculated with Myers-Swiatecki parameters [8], and M^{exp} is the experimental nuclear mass. As regards the other parameter values, we assume $\Delta = 12/\sqrt{A}$, $\varepsilon = 0.24$ and $F_o/\hbar^2 = 73$.

The obtained dependence of $\tilde{a}/A$ on the compound nucleus mass number A is shown in Fig. 7. It is evident that global systematics of $\tilde{a}-$parameter values over actinide region is hardly possible. On the contrary, the isotopic dependences of $\tilde{a}/A$ values seem to be rather smooth. The local systematics of $\tilde{a}-$parameter as

$$\tilde{a}/A = \alpha + \beta A, \tag{11}$$

where α and β are parameters, could be readily obtained. For Th nuclei we get

$$\tilde{a}/A = -1.1320 + 0.00536A; \tag{12}$$

for Pa nuclei

$$\tilde{a}/A = -0.90677 + 0.004319A; \tag{13}$$

for U nuclei

$$\tilde{a}/A = -0.1798 + 0.0012A; \tag{14}$$

for Np nuclei there is only one value for ^{237}Np target nuclide, so

$$\tilde{a}/A = 0.0888 \tag{15}$$

is assumed; for Pu nuclei

$$\tilde{a}/A = -0.723427 + 0.003413A; \tag{16}$$

for Am nuclei

$$\tilde{a}/A = -0.00414 + 0.00038A, \tag{17}$$

for Cm nuclei

$$\tilde{a}/A = -0.0285652 + 0.000476A; \tag{18}$$

for odd Bk nuclei, like in case of Np nuclei, there is only one value for ^{249}Bk nuclide, so we assume

$$\tilde{a}/A = 0.0834A; \tag{19}$$

for Cf nuclei

$$\tilde{a}/A = -71316485 + 0.003180374A; \tag{20}$$

For justified statistical theory calculations it is requested that level density description should reproduce both the average neutron resonance spacing and the observed cumulative number of levels $N^{exp}(U)$. Rather severe problem which one usually deals with in case of actinide nuclei is the fair description of the cumulative number of levels $N^{exp}(U)$ with the $N^{theor}(U)$. Unfortunately, pairing model [7] fails to describe the cumulative number of low-lying levels without introducing additional shift of the excitation energy δ_{shift}. To calculate the level density at the low excitation energy, i.e. just above the last discrete level excitation energy where $N^{exp}(U) \sim N^{theor}(U)$ could be achieved, we employ a Gilbert-Cameron-type constant temperature approach. The constant temperature approximation of level density

$$\rho(U) = dN(U)/dU = T^{-1}\exp((U - U_o)/T) \tag{21}$$

is extrapolated up to the matching point U_c to a phenomenological model by Ignatyuk et al.[7] with the condition

$$U_c = U_o - Tln(T\rho(U_c)). \tag{22}$$

Calculated cumulative number of levels is represented as

$$N(U) = \exp(-U_o/T)\,[\exp(U/T) - 1] \tag{23}$$

Note, that $N(U = 0) = 0$ is the boundary condition at zero excitation energy. In this approach $U_o \simeq -n\triangle_o$, where $\triangle_o$ is the pairing correlation function, $\triangle_o = 12/\sqrt{A}$, A is the mass number, i.e., U_o has the meaning of the odd-even energy shift (see definition of condensation E_{cond} and excitation U energies above). The value of nuclear temperature parameter T is obtained by the matching conditions at the excitation energy U_c.

In current approach the modelling of total level density

$$\rho(U) = K_{rot}(U)K_{vib}(U)\frac{\omega_{qp}(U)}{\sqrt{2\pi}\sigma} = T^{-1}\exp((U - U_o)/T) \tag{24}$$

in Gilbert-Cameron-type approximation looks like a simple renormalization of quasiparticle state density $\omega_{qp}(U)$ at excitation energies $U < U_c$.

Figures 8 - 58 demonstrate the description of cumulative plots of low-lying levels for Th, Pa, U, Np, Pu, Am, Cm, Bk and Cf nuclei within current approach. Histogram plots were obtained using ENSDF data, straight solid lines are model fits.

Cumulative plots for even Th nuclei ^{228}Th, ^{230}Th and ^{232}Th look very similar to each other, while those for ^{226}Th and ^{234}Th seem to be rather incomplete. Using matching energy U_c = 4.4 MeV, defined for ^{230}Th, also for ^{228}Th and ^{232}Th we could fit relevant cumulative plots, main level density parameter $\tilde{a}$ being defined by systematics. Cumulative plots for ^{226}Th and ^{234}Th seem to reveal missing of levels at very low excitation energies, so U_c = 4.4 MeV should be used.

Cumulative plots for odd Th nuclei ^{231}Th and ^{233}Th look very similar to each other, they are fitted assuming matching energy U_c = 3.6 MeV. Cumulative plot for ^{229}Th is much more steeper, so using U_c= 3.6 MeV also for ^{229}Th we would strongly underestimate the observed number of levels. To fit cumulative plot of ^{229}Th nuclide, value of U_c should be increased up to 4.8 MeV, main level density parameter $\tilde{a}$ being defined by systematics.

Cumulative plots for even U nuclides ^{232}U, ^{234}U, ^{236}U and ^{238}U look very similar to each other. They could be fitted with U_c= 4.4 MeV, except for ^{238}U where U_c= 4.0 MeV is assumed. In case of ^{232}U, a value of U_c= 4.4 MeV is accepted, main level density parameter $\tilde{a}$ being defined by systematics.

In case of odd U nuclei steepest cumulative plot is observed for ^{235}U nuclide. For ^{233}U and ^{237}U nuclides difference is only slight, so values of U_c = 2.8 MeV U_c = 2.6 MeV, respectively, are used . However, for ^{235}U nuclide we should increase U_c up to 3.8 MeV. For ^{239}U nuclide missing of levels starts at rather low excitation energy $U \sim 0.25$ MeV, which is predicted if value of U_c = 2.8 MeV is accepted.

Among even Pu nuclides, the cumulative plot for ^{240}Pu seems to be the steepest, value of U_c = 4.0 MeV is estimated. For ^{242}Pu nuclide U_c = 3.6 MeV is obtained. For ^{244}Pu we assume U_c = 3.6 MeV, that means missing of levels starts at excitations as low as $\sim$ 0.6 MeV. In case of ^{238}Pu nuclide U_c = 3.6 MeV is accepted, main level density parameter $\tilde{a}$ being defined by systematics.

Among odd Pu nuclides, the cumulative plot for ^{241}Pu seems to be the steepest, value of U_c = 2.8 MeV is assumed, for other Pu nuclei U_c value decreases from 2.4 MeV for ^{239}Pu down to 1.6 MeV for ^{245}Pu, as cumulative plot goes less steep. It is difficult to conclude whether it is a real effect or just a consequence of level missing. In case of ^{237}Pu nuclide U_c = 2.8 MeV is accepted, main level density parameter $\tilde{a}$ being defined by systematics.

Low-lying level schemes of even Cm nuclides seem to be rather incomplete, consequently cumulative plots generally can not be used for constant temperature parameter definition. The only exception is ^{246}Cm. However, even in that case low-lying level scheme should be complemented with additional levels of quadrupole and octupole vibrational bands [12]. Then, a value of matching energy U_c = 3.4 MeV is extracted, for other even nuclides this value of matching energy predicts severe missing of levels at excitation as low as 0.6 MeV. The same is the case for ^{250}Cf nuclide, when U_c = 3.4 MeV.

In case of odd Cm nuclei constant temperature parameters are also correlated with cumulative plot trends. For ^{243}Cm there is a distinct anomaly as compared with other Cm nuclei, matching energy U_c being estimated as 4.4 MeV. The number of levels is defined mainly by odd-even energy shift U_o, absolute value of which increases with matching energy U_c increase. If not for the ^{243}Cm, U_c would increase smoothly from U_c = 2.2 MeV for ^{245}Cm, U_c = 2.8 MeV for ^{247}Cm up to U_c = 3.2 MeV for ^{249}Cm. As regards nuclear temperature parameter T values, there is a correlated slightly-increasing trend. For odd ^{249}Cf U_c = 2.8 MeV, while for ^{251}Cf nuclide U_c = 3.2 MeV could be used.

For $Z-$odd Pa, Np, Am and Bk nuclei situation is more complex than in case of $Z-$ even nuclei. Specifically, neutron resonance spacings are available mostly for odd-odd compound nuclei, which cumulative plots seem to be rather incomplete. On the other hand, for $Z-$odd, $N-$even compound nuclei cumulative plots look reasonable, while level density parameters could be estimated only based on systematic trends, except ^{243}Am compound nuclide. Namely, cumulative plots for ^{231}Pa and ^{233}Pa nuclides could be described assuming U_c = 4.4 MeV. Cumulative plots for ^{235}Np, ^{237}Np and ^{239}Np are described assuming U_c = 3.6 MeV. Cumulative plots for ^{239}Am, ^{241}Am, ^{243}Am and ^{245}Am could be described assuming $U_c = 3.6$ MeV, and for ^{243}Am description seems to be the best. The same value of $U_c = 3.6$ MeV is used for ^{249}Bk nuclide. For $Z-$odd, $N-$odd nuclei situation is unsatisfactory. Cumulative plots of ^{238}Np, ^{236}Np, ^{242}Am, ^{244}Am, ^{248}Bk and ^{250}Bk cannot be fitted with current approach, mainly because we define odd-even excitation energy correction as $2\triangle_o$. Figure 44 for ^{242}Am shows that fitting of cumulative plot is impossible even decreasing U_c value from 2.4 MeV down to 0.8 MeV.

Table 2 Constant temperature model parameters

^AX	U_c, MeV	U_o, MeV	T, MeV	^AX	U_c, MeV	U_o, MeV	T, MeV
^{226}Th	4.4	-.15693	0.41725	^{240}Pu	4.0	0.09992	0.38691
^{228}Th	4.4	-.17373	0.40806	^{241}Pu	2.8	-.75741	0.37538
^{229}Th	4.8	-1.2239	0.37599	^{242}Pu	3.6	0.01559	0.37200
^{230}Th	4.4	-.1700	0.39709	^{243}Pu	2.0	-.48771	0.33801
^{231}Th	3.6	-.94750	0.39020	^{244}Pu	3.6	0.47551	0.35942
^{232}Th	4.4	-.15538	0.38606	^{245}Pu	1.6	-.34261	0.31498
^{233}Th	3.6	-.92613	0.37977	^{239}Am	3.6	-.96889	0.40732
^{234}Th	4.4	-0.13581	0.37542	^{240}Am	2.4	-1.6480	0.39682
^{231}Pa	4.4	-1.1698	0.42322	^{241}Am	3.6	-.97413	0.40495
^{233}Pa	4.4	-1.1911	0.41522	^{242}Am*	2.4	-1.6457	0.39345
^{232}U	4.4	-.18277	0.39966	^{243}Am*	3.6	-.97830	0.40274
^{233}U	2.8	-.73554	0.37578	^{244}Am *	2.4	-1.6425	0.39028
^{234}U	4.4	-.19143	0.40018	^{245}Am	3.6	-.98497	0.39835
^{235}U	3.8	-1.0275	0.40314	^{243}Cm	4.4	-1.1659	0.41572
^{236}U	4.4	-.19024	0.39320	^{244}Cm*	3.4	0.03342	0.37599
^{237}U	2.6	-.68059	0.36704	^{245}Cm	2.2	-.61989	0.36197
^{238}U	4.0	-.06227	.37575	^{246}Cm*	3.4	0.03277	0.37307
^{239}U	2.8	-.71107	0.36291	^{247}Cm*	2.8	-.77480	0.37599
^{235}Np	3.6	-.97315	0.40661	^{248}Cm	3.4	0.03185	0.37035
^{236}Np	2.4	-1.6508	0.39572	^{249}Cm	3.2	-.88400	0.38488
^{237}Np	3.6	-.97572	0.40480	^{248}Bk	2.4	-1.6367	0.39377
^{238}Np	2.4	-1.6483	0.39394	^{249}Bk	3.6	-.97173	0.40172
^{239}Np	3.6	-.97862	0.40252	^{250}Bk	2.4	-1.6375	0.38985
^{237}Pu	2.8	-.77813	0.38776	^{249}Cf	2.8	-.69672	0.35037
^{238}Pu	3.6	.00022	0.38454	^{250}Cf	3.4	0.00141	0.37941
^{239}Pu	2.4	-.65665	0.36847	^{251}Cf	3.2	-.76588	0.34349

Figures 59, 60 and 61 show evident systematic trends for constant temperature model parameters U_c, U_o and T. Generally, there is a grouping of matching energy U_c values for even-even, odd and odd-odd nuclei (see Fig. 59), although there are distinct fluctuations for nuclei with relatively steep (^{243}Cm) or flat (^{245}Pu) cumulative plots. In latter case it might be due to severe missing of levels. Odd-even energy shift U_o values have pronounced grouping with particularly noticeable irregularity for odd Pu nuclei (see Fig. 60). Nuclear temperature parameter T exhibits the correlated fluctuations with those of U_c, but there is no as distinct odd-even grouping of values (see Fig. 61). Instead, there is a smooth decreasing trend of temperature T values for isotopes with increase of the number of neutrons N.

Figure 62 demonstrates the ratio of calculated neutron resonance spacing $D_{syst.}$ to the estimated from measured data neutron resonance spacing D_{exp}. In general, the discrepancy is quite comparable with attributed errors of D_{exp}. That means $\tilde{a}$−parameter systematics could be used for neutron resonance spacing estimates and subsequent description of low-lying number of levels.

Current values of constant temperature model parameters U_c, U_o and T are generally discrepant with recent estimates [13] made based solely on cumulative plot fits. Producing fits of cumulative plots, these parameters might lead to incorrect estimates of the cut-off energy, above which appreciable missing of levels starts. Another obvious consequence is incorrect extrapolation of level density shape even in a few-MeV excitation energy range, since nuclear temperature T values fluctuate wildly. In present approach constant temperature model parameter T is strictly correlated with level density shape, extrapolated from the excitation energy equal to the binding energy of the neutron to the matching point U_c. Another constant temperature model parameter U_o is not much different from the odd-even correction to the excitation energy, used in the level density model. Smooth trends revealed in this parameter values make them particularly suitable for extrapolations to lower and higher mass nuclides. However, one should be cautious, since fluctuations are still possible.

3 Concluding Remarks

Neutron resonance spacing data measured for actinides were analyzed to obtain the level density parameters for Th - Cf. The level density is represented by constant temperature and Fermi gas models. The systematics of the $\tilde{a}$ parameters was obtained for each element. The parameters for the constant temperature model revealed some systematic trend. The parameters and systemtics obtained are useful for nuclear data evaluation for actinides.

Acknowledgments

This work was started within Project B-03 "Actinide Nuclear Data Evaluation" of International Science and Technology Center (Moscow, Russia) and completed during the stay of one of the authors (V.M. Maslov) at JAERI under the framework of the Foreign Scientists Invitation Program of JAERI. One of the authors (V.M. Maslov) wishes to thank the members of the JAERI Nuclear Data Center for helpful discussions. Partial support of International Atomic Energy Agency (Vienna, Austria) under Research Contract 9503 is acknowledged by Yu.V. Porodzinskij.

References

[1] Porodzinskij Yu.V., Sukhovitskij E.Sh. and Maslov V.M., Proc. Int. Conf. Nucl. Data for Sci. and Technology, Trieste, Italy, May 19-23, 1997, p. 937.

[2] Porodzinskij Yu.V., Sukhovitskij E.Sh., Proc. of ISTC Workshop on Nuclear Data of Minor Actinides, May 27-31,1996, JAERI, Tokai, Japan, JAERI-Conf, 97-001, p.34.

[3] Porter C.E. and Thomas R.G., Phys. Rev., 104, 483 (1956).

[4] Wigner E.P., in Proc. Conf. Appl. Math. (Toronto,1959), p.483.

[5] Maslov V.M., Porodzinskij Yu.V., Sukhovitskij E.Sh., Klepatskij A.B., Morogovskij G.B. and Y. Kikuchi, Proc. International Conference on the Physics Reactors, September 16-20, 1996, Mito, Ibaraki, Japan, vol.3, p.F1.

[6] Maslov V.M., Porodzinskij Yu.V., Sukhovitskij E.Sh., Morogovskij G.B. Proc. Int. Conf. Nucl. Data for Sci. and Technology, Trieste, Italy, May 19-23, 1997, p.1317.

[7] Ignatjuk A.V., Istekov K.K., Smirenkin G.N. Sov. J. Nucl. Phys. 29, 450 (1979)

[8] Myers W.O., Swiatecky W.J., Ark. Fyzik, 36, 243 (1967).

[9] Mughabghab S.F.: "Neutron Cross Sections, v1, part B", Academic Press (1984).

[10] Ignatyuk A.V., private communication.

[11] Evaluated Nuclear Structure Data File, 1997.

[12] Maslov V.M., Porodzinskij Yu.V., Sukhovitskij E.Sh. et al., INDC(BLR)-4, 1996, IAEA, Vienna.

[13] Belgya T., Molnar G., Fazekas B. and Östör J. INDC(NDS)-367, IAEA, Vienna, 1997.

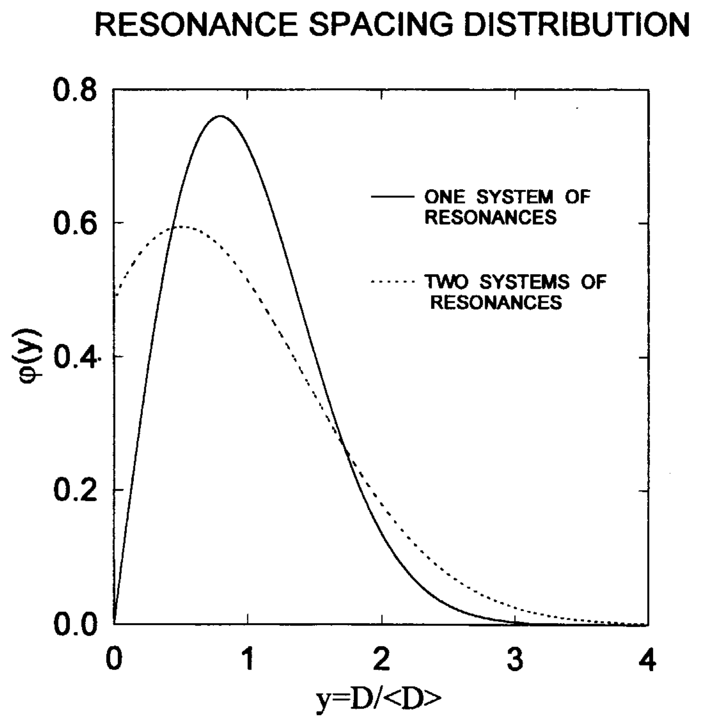

Fig. 1 Comparison of level spacing distributions with one and two systems of resonances.

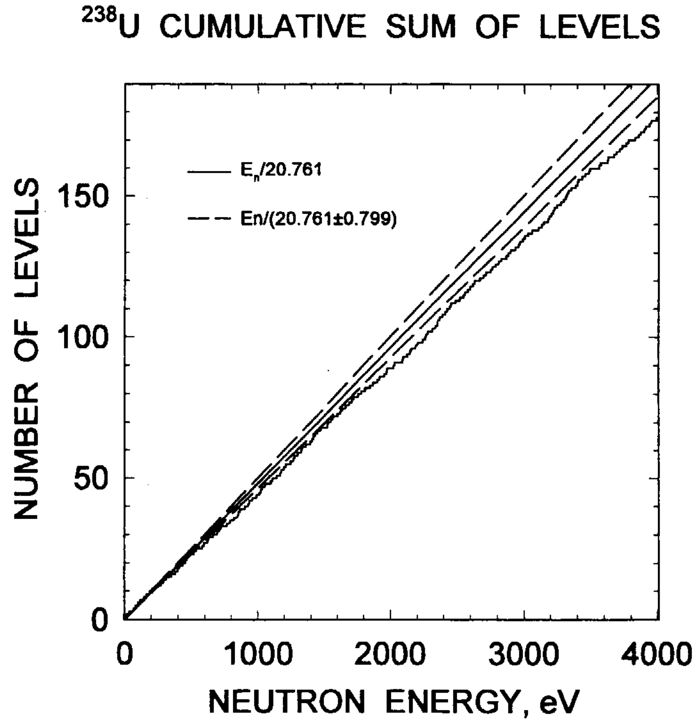

Fig. 2 Cumulative sum of neutron resonance levels for ^{238}U target.

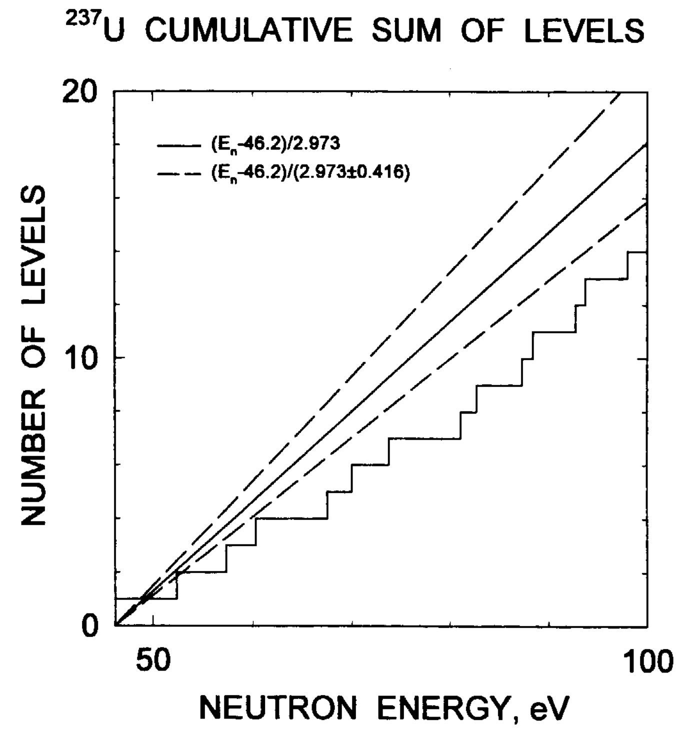

Fig. 3 Cumulative sum of neutron resonance levels for ^{237}U target.

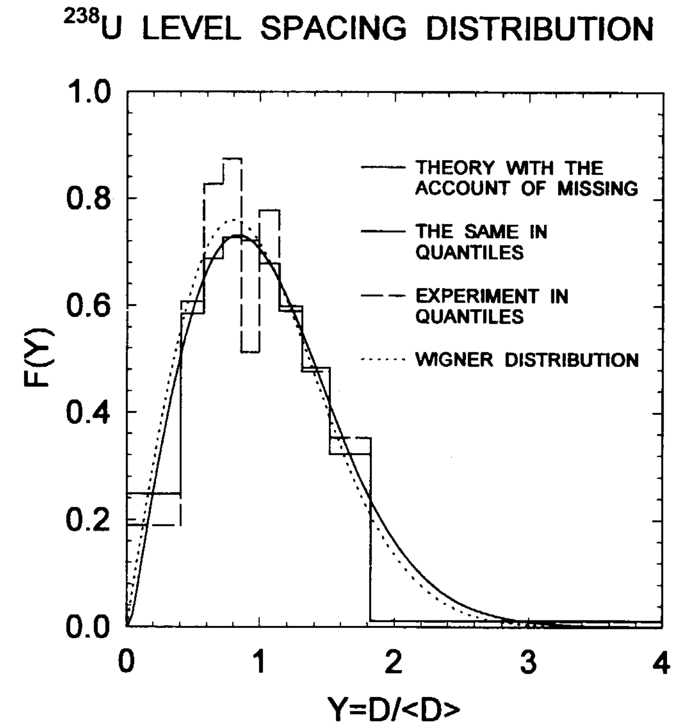

Fig. 4 Neutron resonance spacing distribution of ^{238}U.

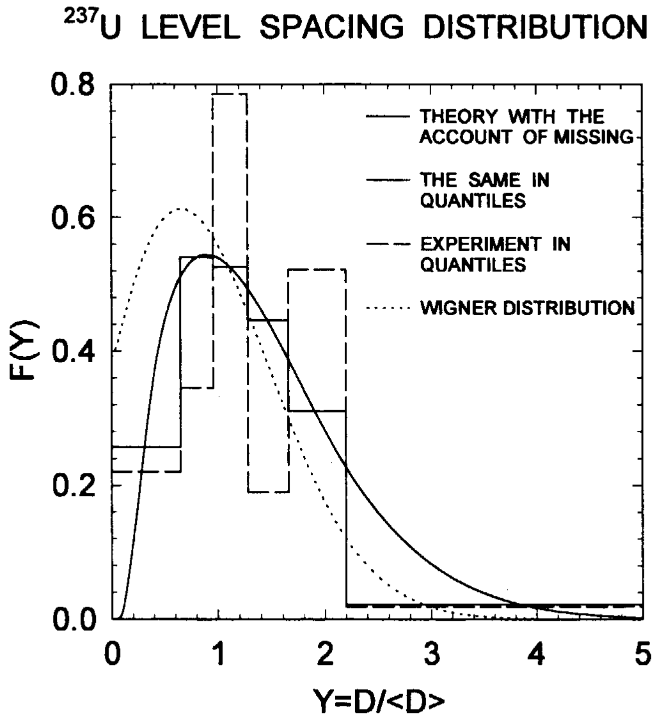

Fig. 5 Neutron resonance spacing distribution of ^{237}U.

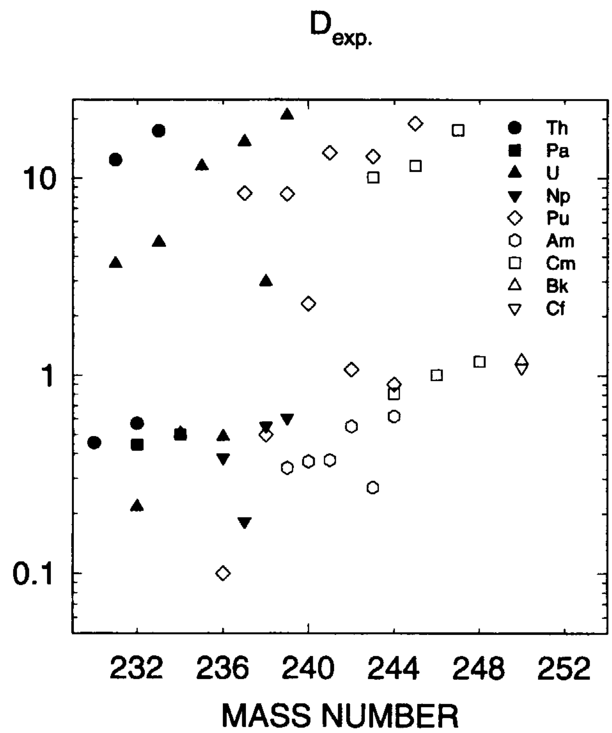

Fig. 6 Neutron resonance spacing data.

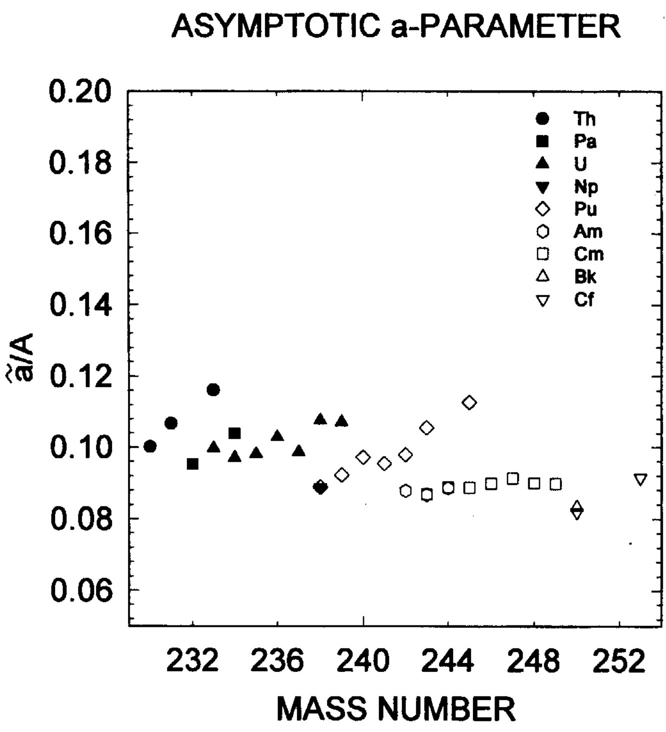

Fig. 7 Main parameter of level density $\tilde{a}$.

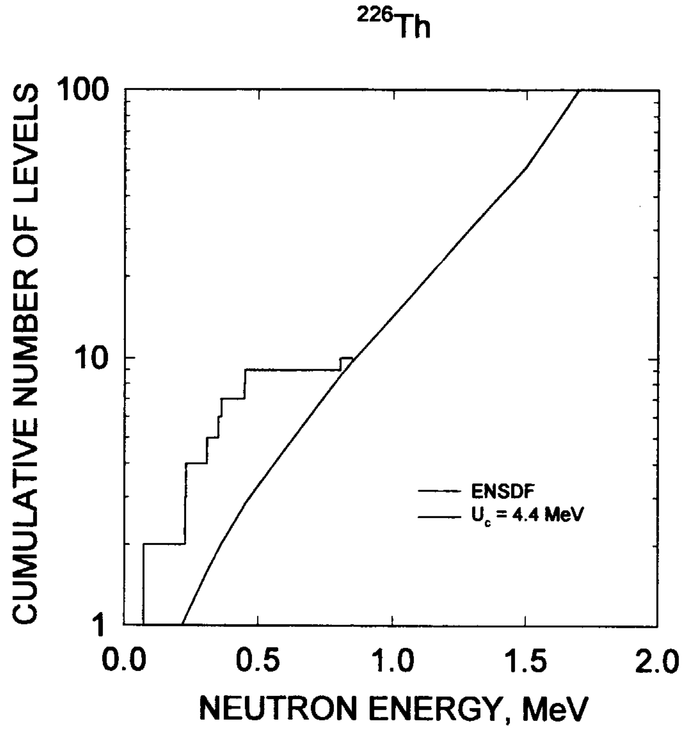

Fig. 8 Cumulative sum of low-lying levels of ^{226}Th.

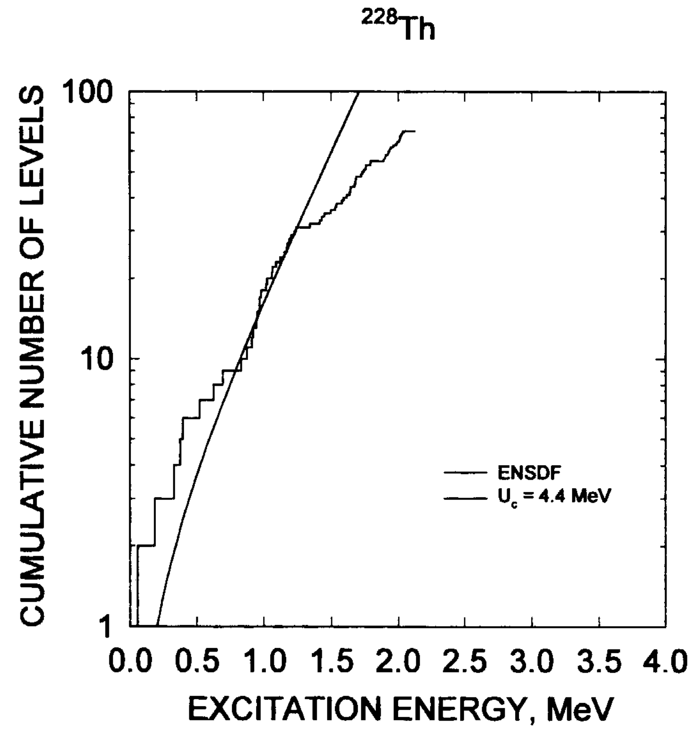

Fig. 9 Cumulative sum of low-lying levels of ^{228}Th.

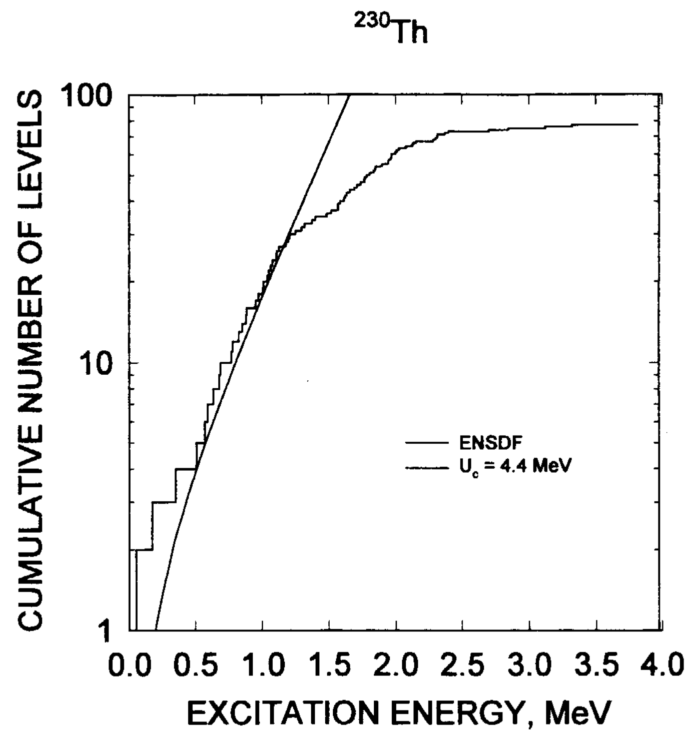

Fig. 10 Cumulative sum of low-lying levels of ^{230}Th.

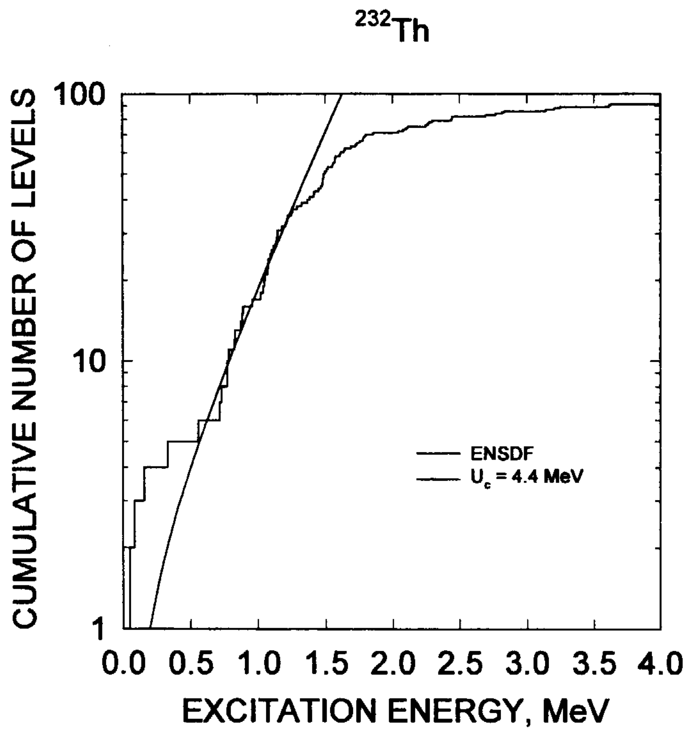

Fig. 11 Cumulative sum of low-lying levels of ^{232}Th.

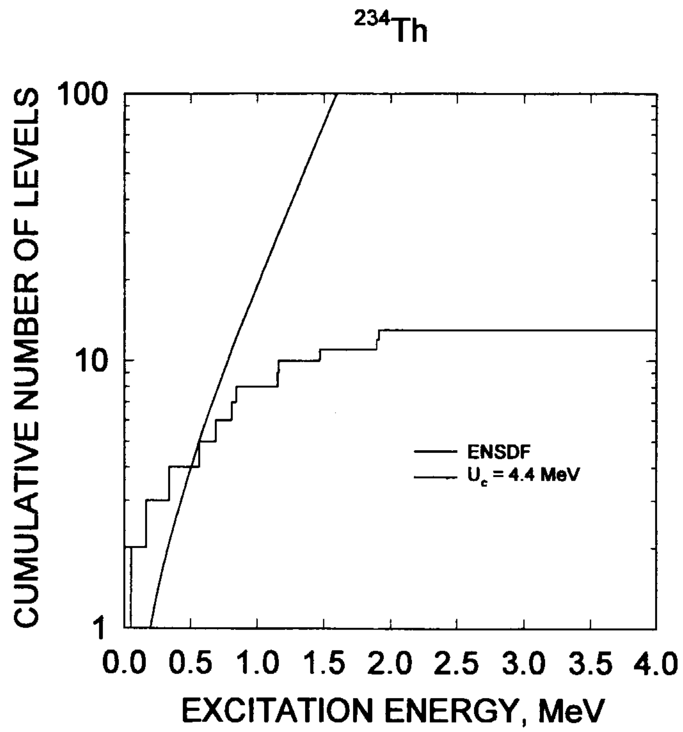

Fig. 12 Cumulative sum of low-lying levels of ^{234}Th.

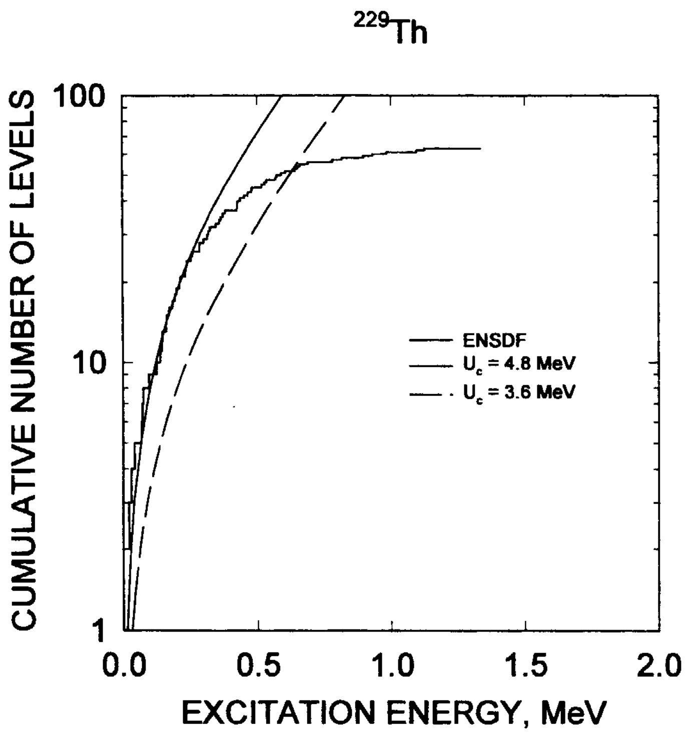

Fig. 13 Cumulative sum of low-lying levels of ^{229}Th.

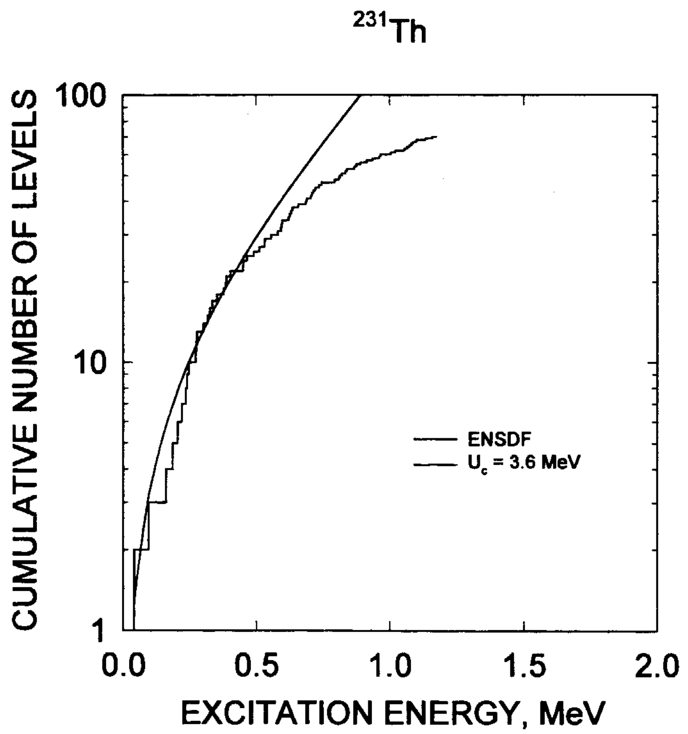

Fig. 14 Cumulative sum of low-lying levels of ^{231}Th.

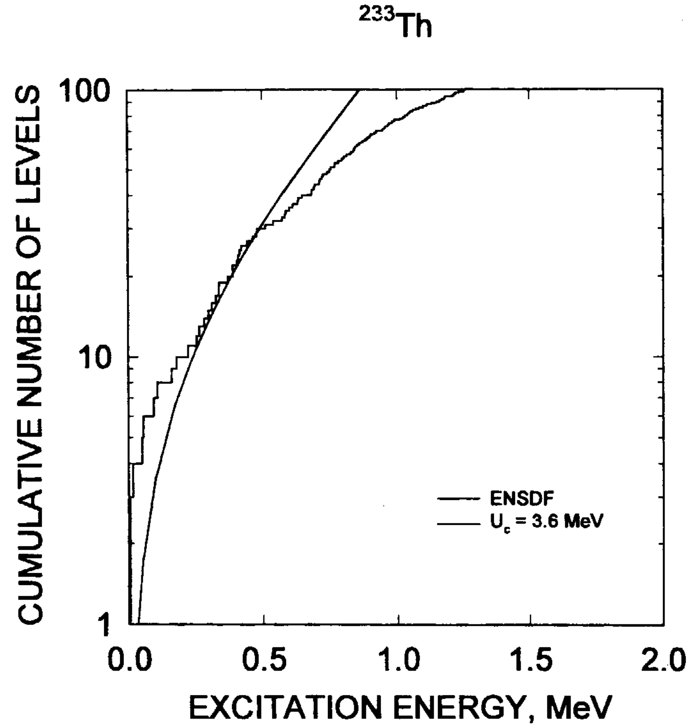

Fig. 15 Cumulative sum of low-lying levels of ^{233}Th.

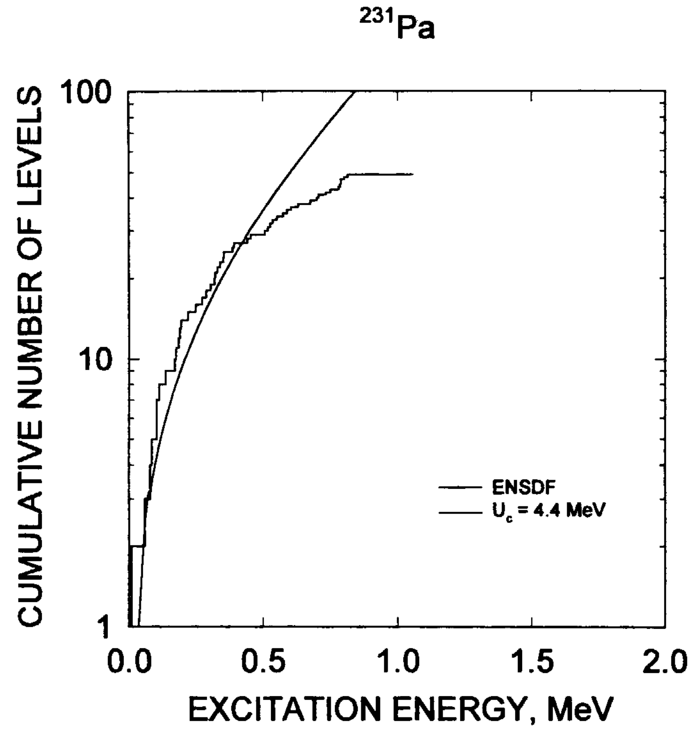

Fig. 16 Cumulative sum of low-lying levels of ^{231}Pa.

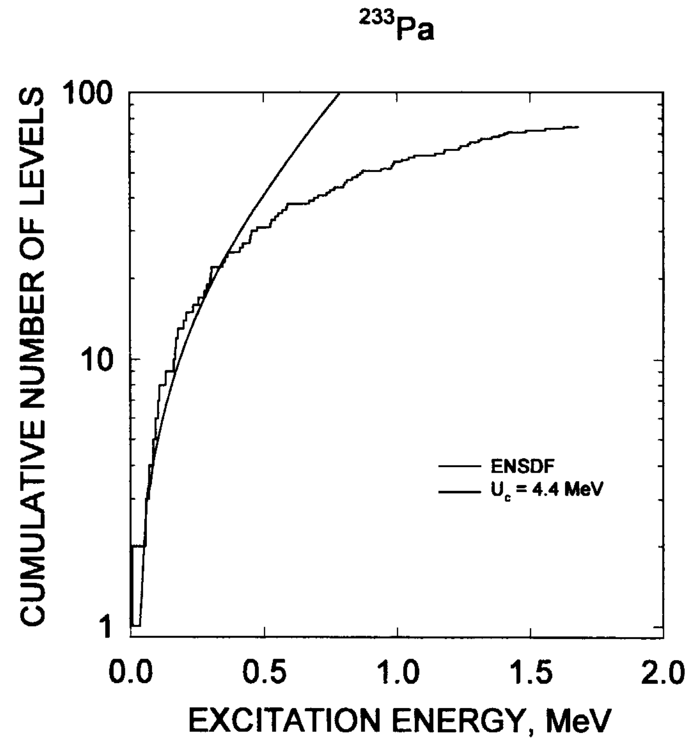

Fig. 17 Cumulative sum of low-lying levels of ^{233}Pa.

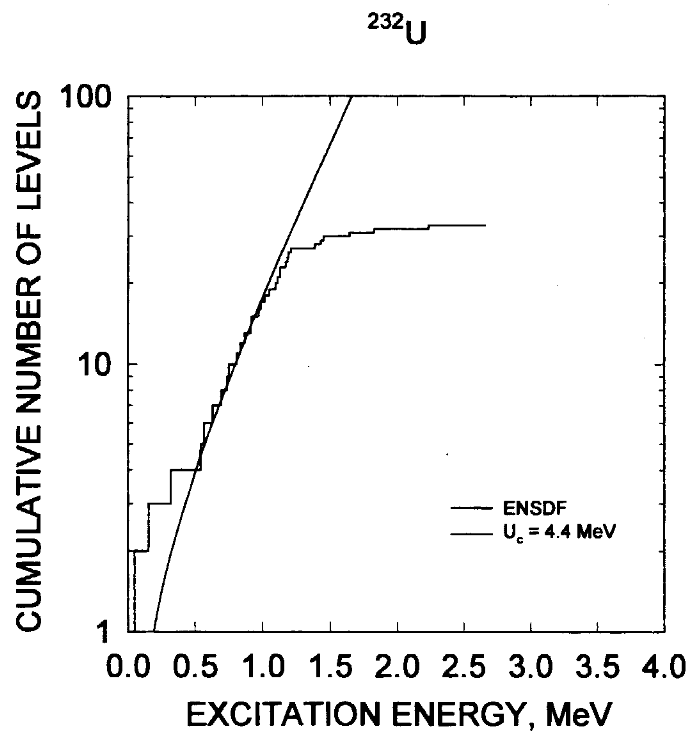

Fig. 18 Cumulative sum of low-lying levels of ^{232}U.

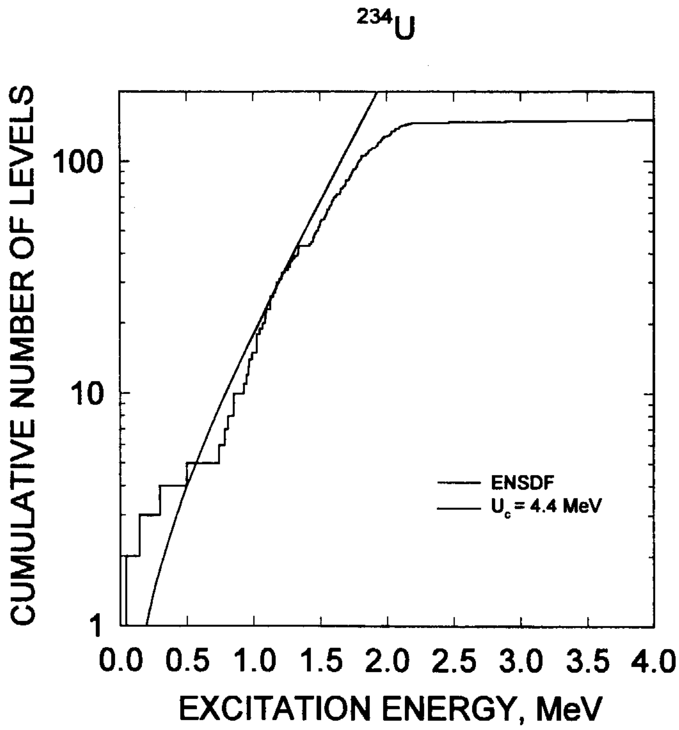

Fig. 19 Cumulative sum of low-lying levels of ^{234}U.

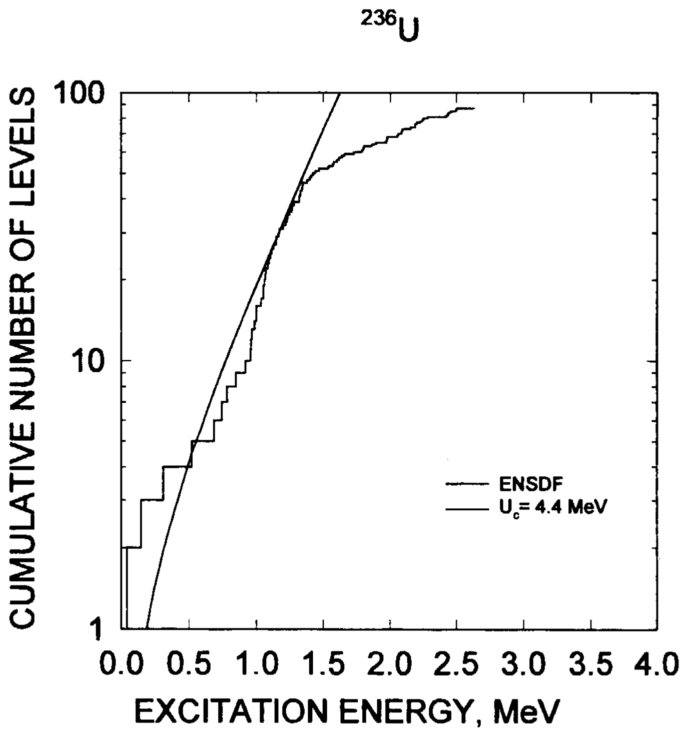

Fig. 20 Cumulative sum of low-lying levels of ^{236}U.

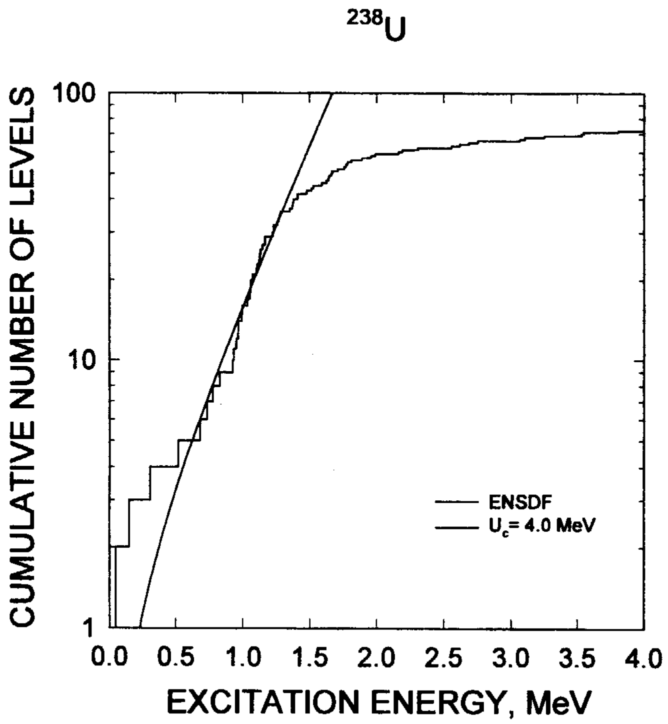

Fig. 21 Cumulative sum of low-lying levels of ^{238}U.

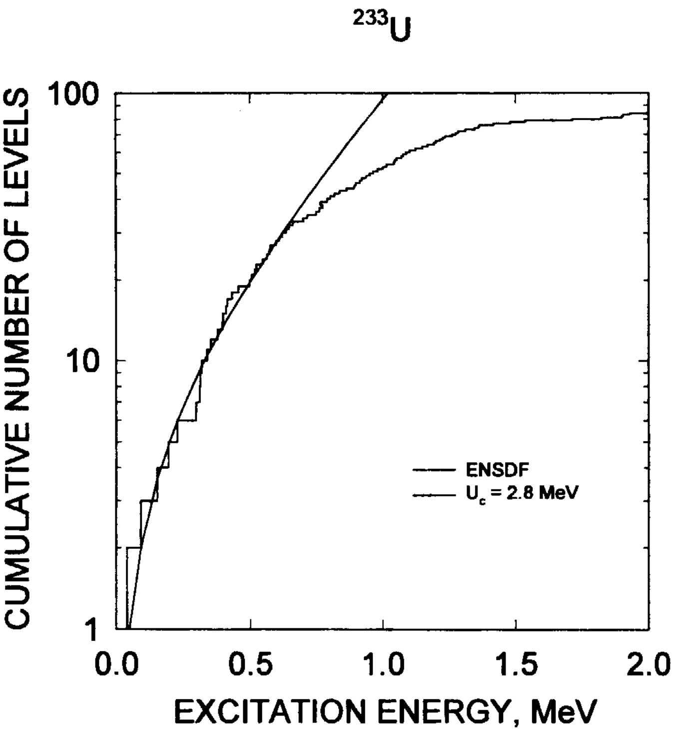

Fig. 22 Cumulative sum of low-lying levels of ^{233}U.

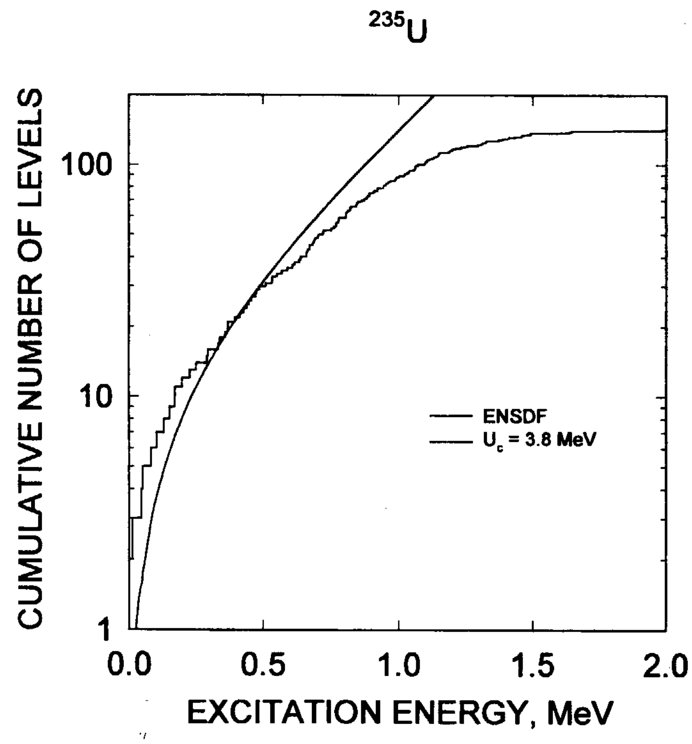

Fig. 23 Cumulative sum of low-lying levels of ^{235}U.

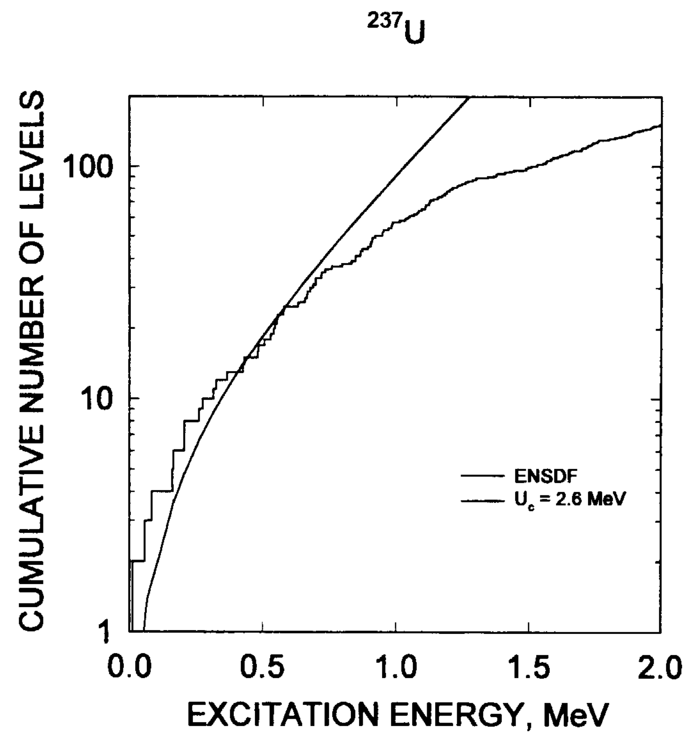

Fig. 24 Cumulative sum of low-lying levels of ^{237}U.

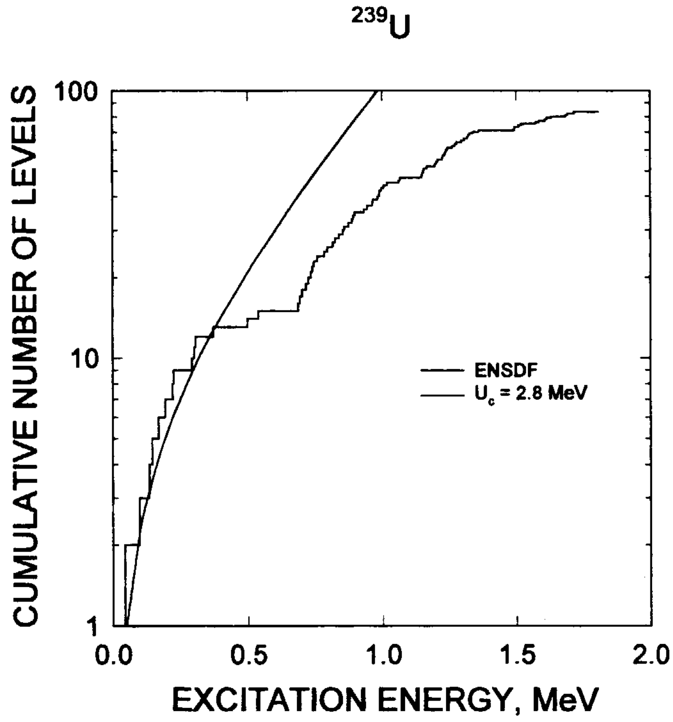

Fig. 25 Cumulative sum of low-lying levels of ^{239}U.

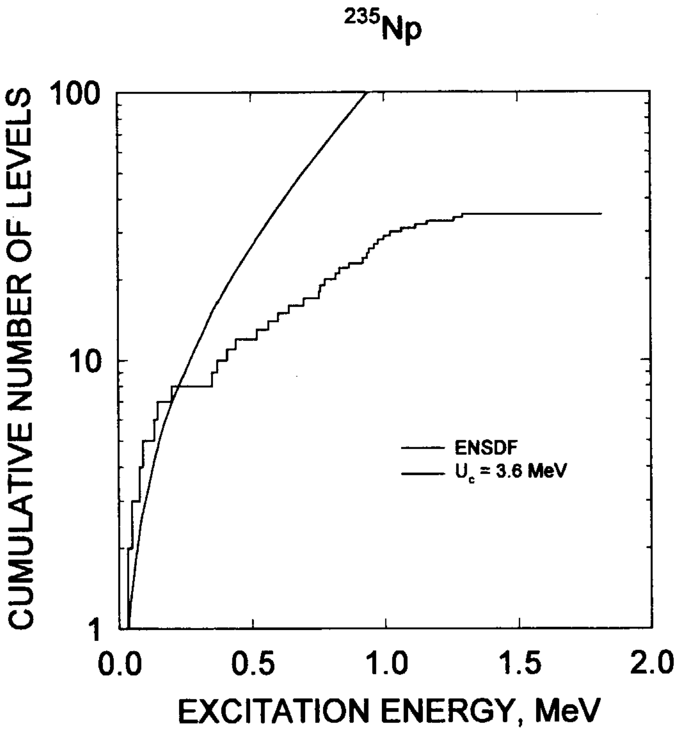

Fig. 26 Cumulative sum of low-lying levels of ^{235}Np.

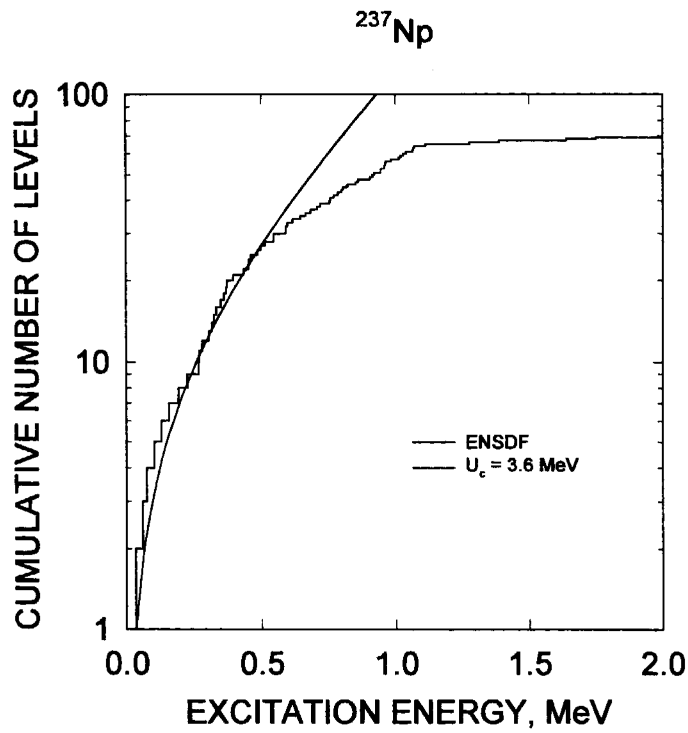

Fig. 27 Cumulative sum of low-lying levels of ^{237}Np.

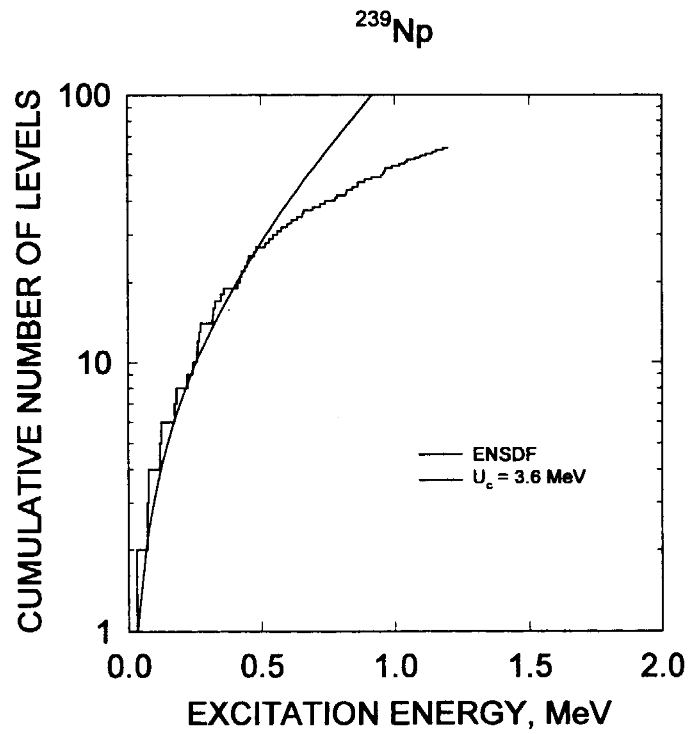

Fig. 28 Cumulative sum of low-lying levels of ^{239}Np.

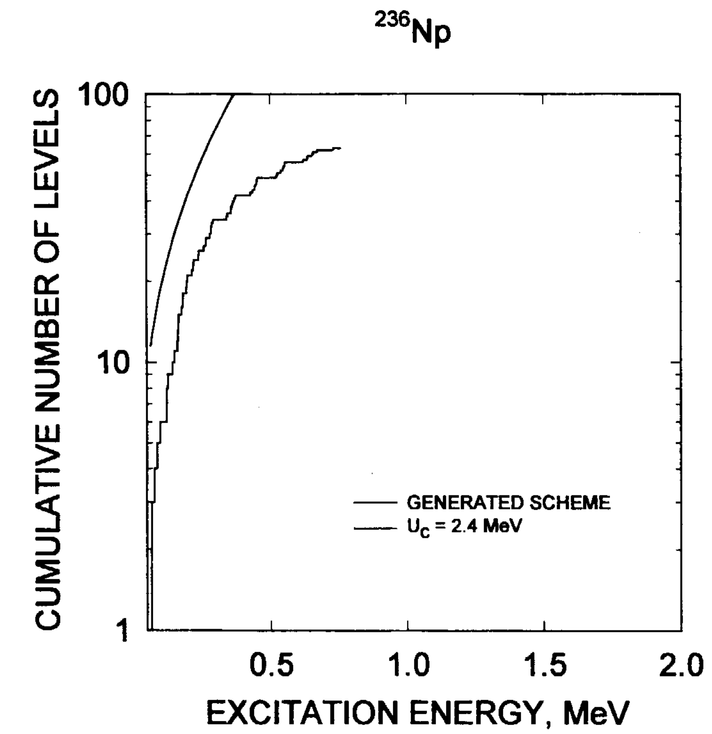

Fig. 29 Cumulative sum of low-lying levels of ^{236}Np.

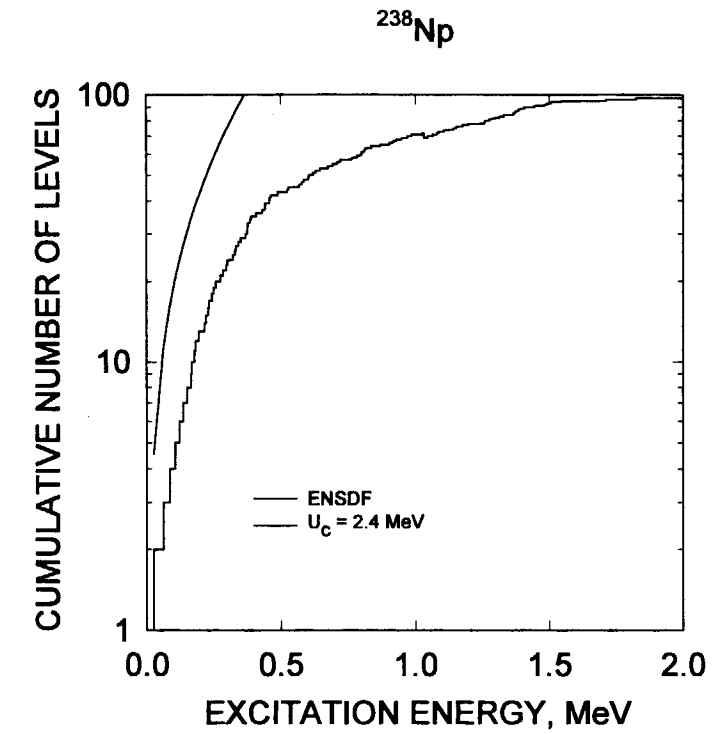

Fig. 30 Cumulative sum of low-lying levels of ^{238}Np.

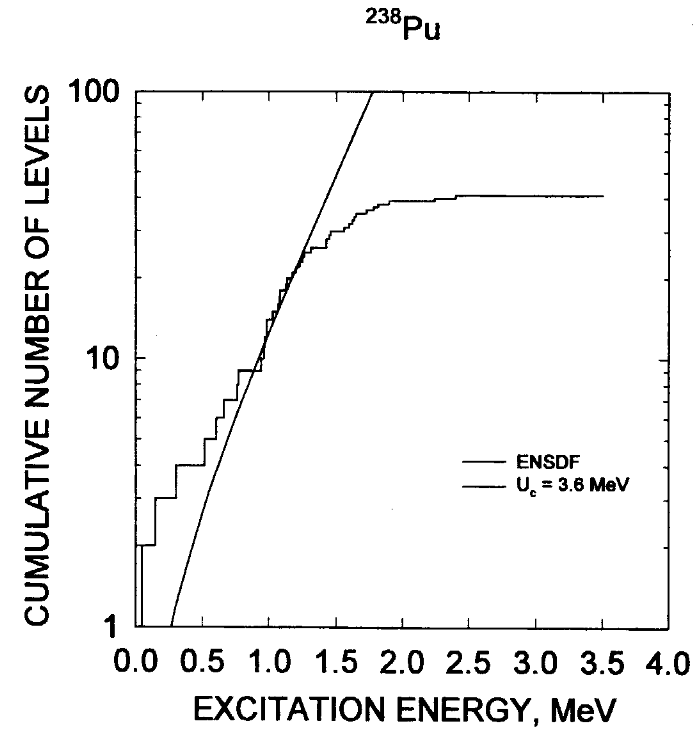

Fig. 31 Cumulative sum of low-lying levels of ^{238}Pu.

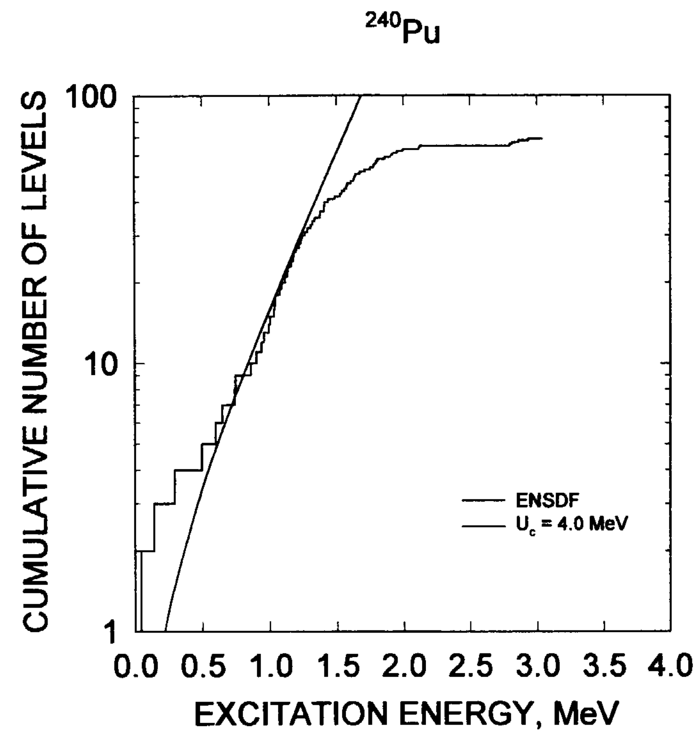

Fig. 32 Cumulative sum of low-lying levels of ^{240}Pu.

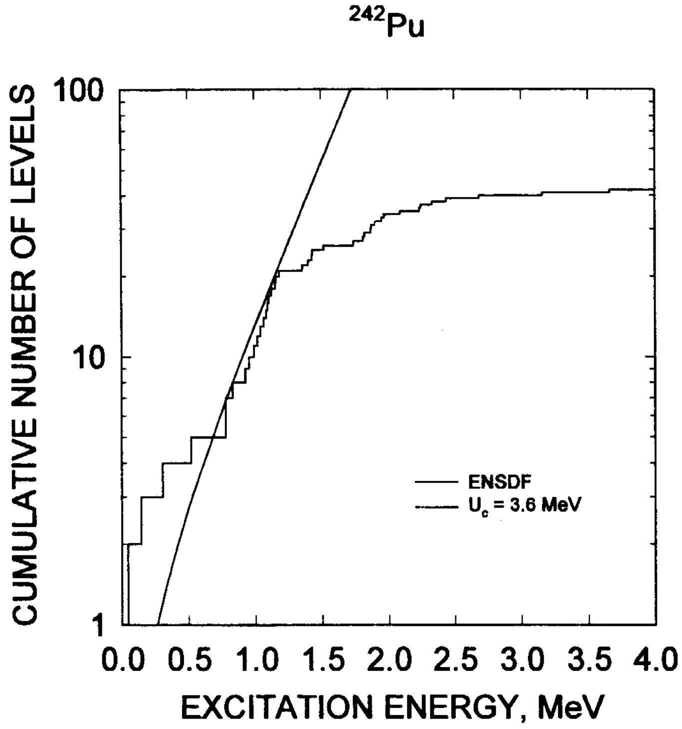

Fig. 33 Cumulative sum of low-lying levels of ^{242}Pu.

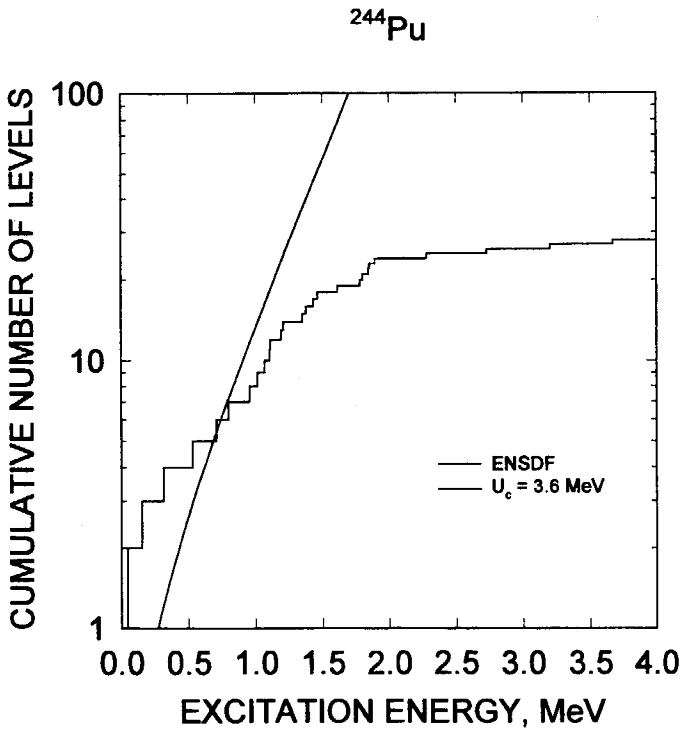

Fig. 34 Cumulative sum of low-lying levels of ^{244}Pu.

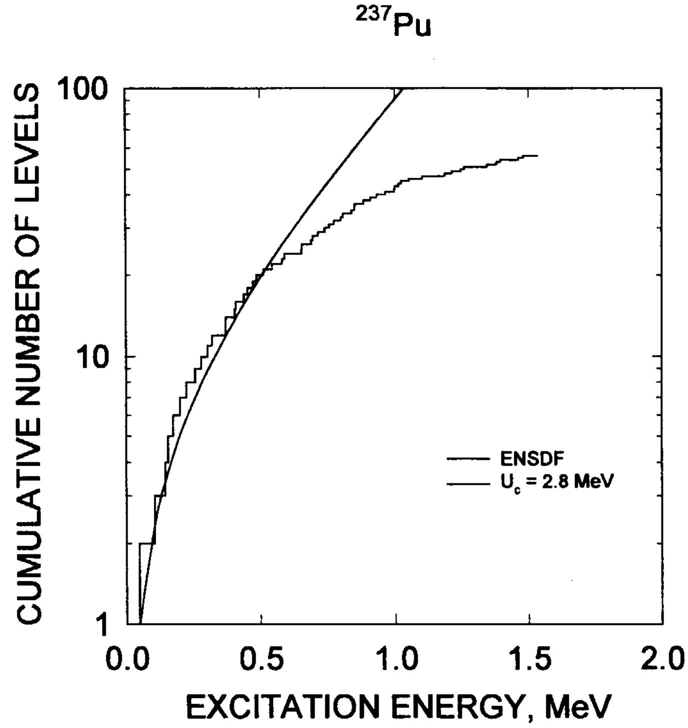

Fig. 35 Cumulative sum of low-lying levels of ^{237}Pu.

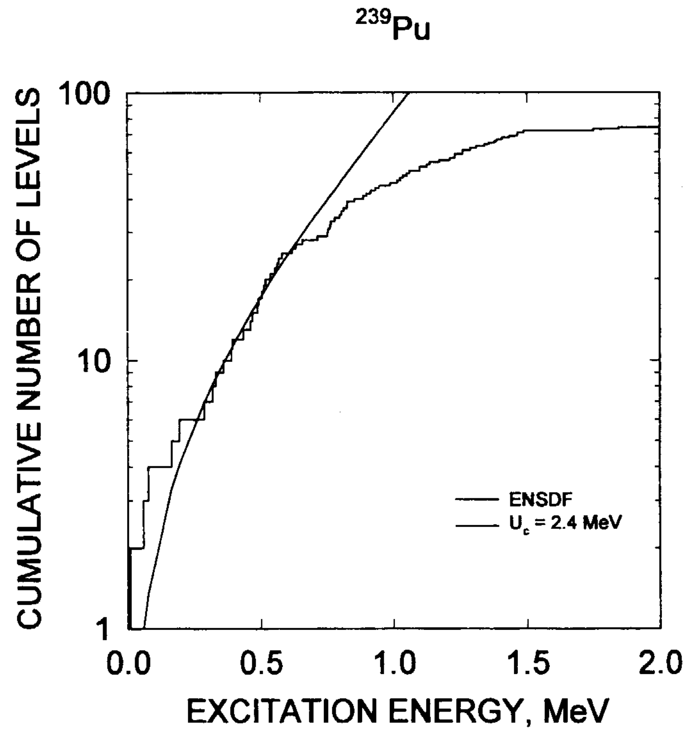

Fig. 36 Cumulative sum of low-lying levels of ^{239}Pu.

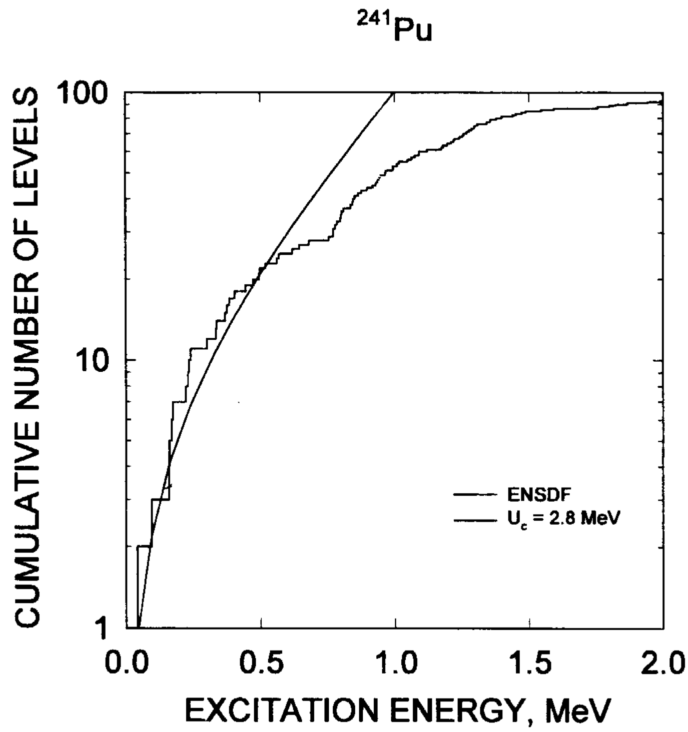

Fig. 37 Cumulative sum of low-lying levels of ^{241}Pu.

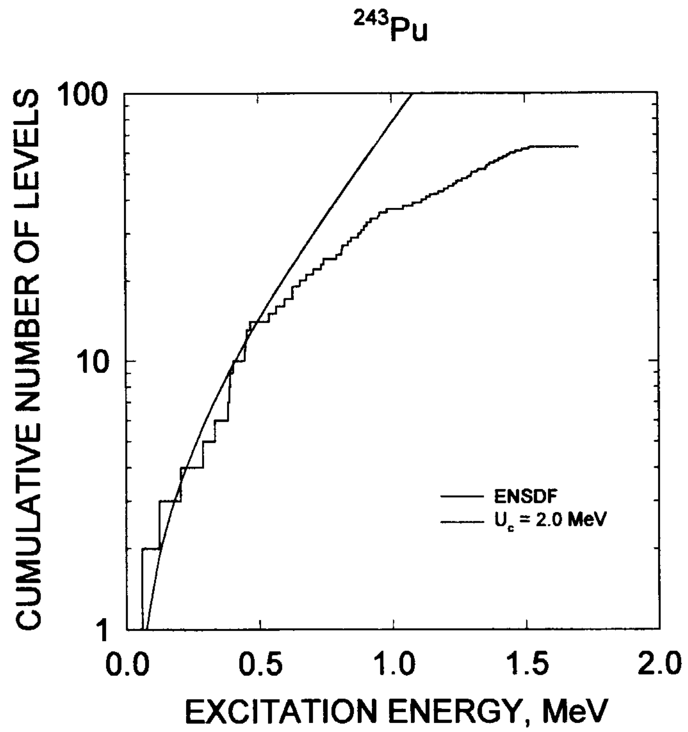

Fig. 38 Cumulative sum of low-lying levels of ^{243}Pu.

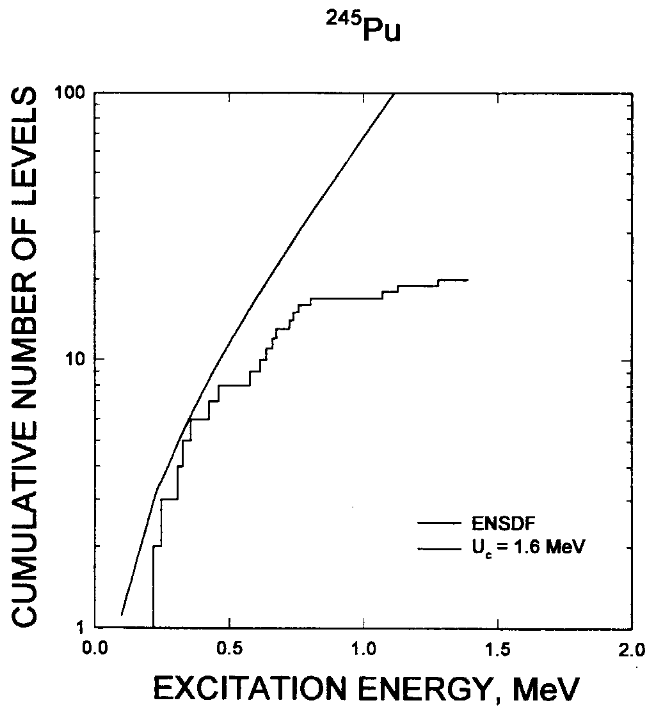

Fig. 39 Cumulative sum of low-lying levels of ^{245}Pu.

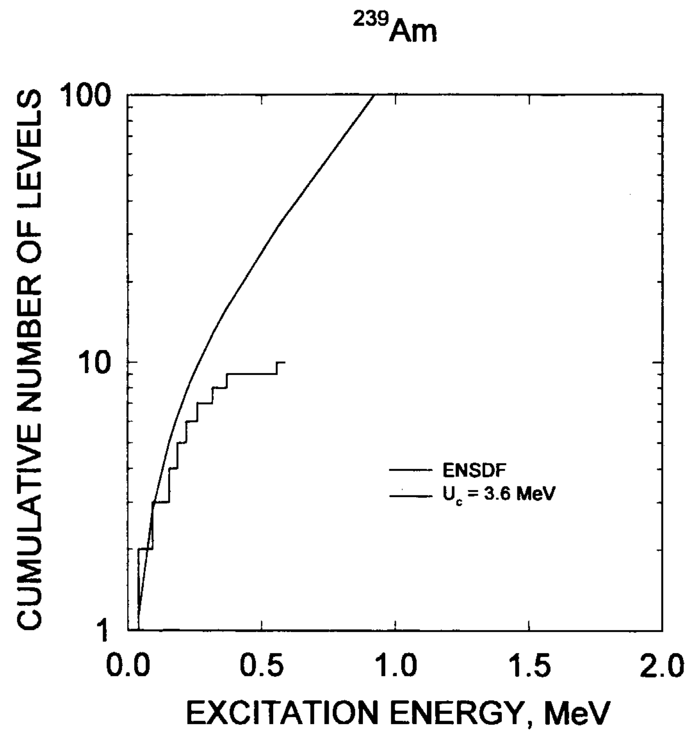

Fig. 40 Cumulative sum of low-lying levels of ^{239}Am.

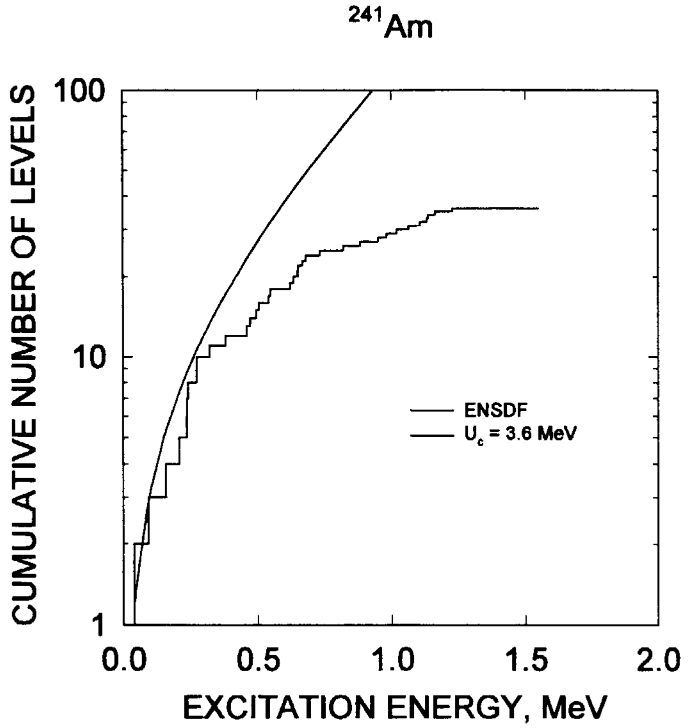

Fig. 41 Cumulative sum of low-lying levels of ^{241}Am.

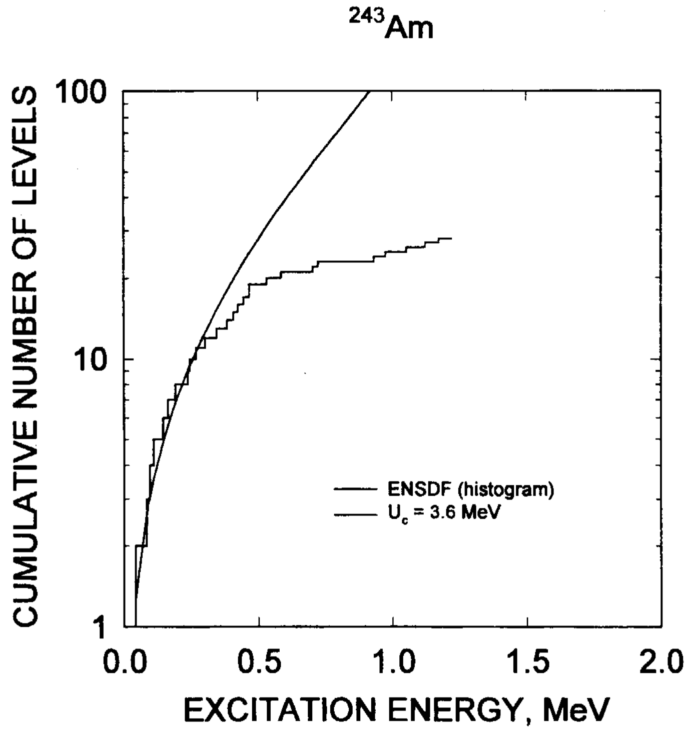

Fig. 42 Cumulative sum of low-lying levels of ^{243}Am.

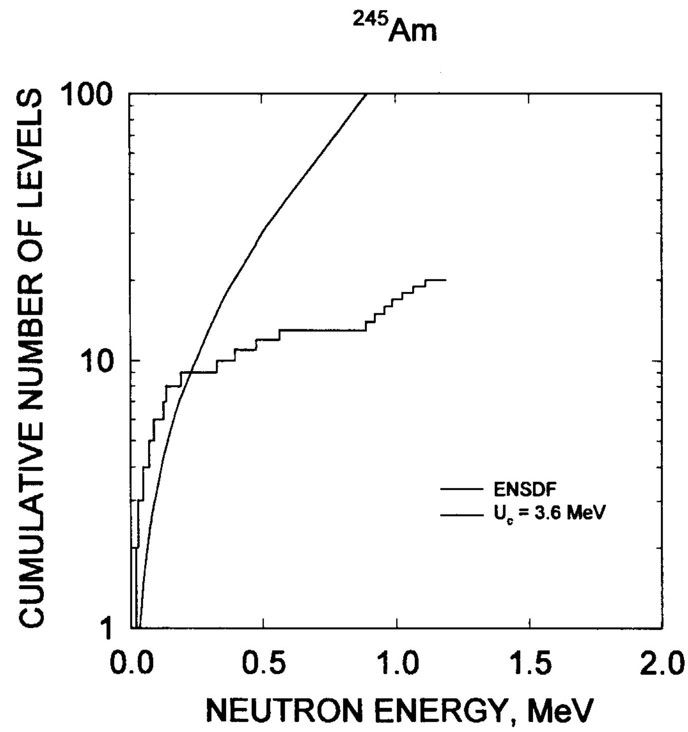

Fig. 43 Cumulative sum of low-lying levels of ^{245}Am.

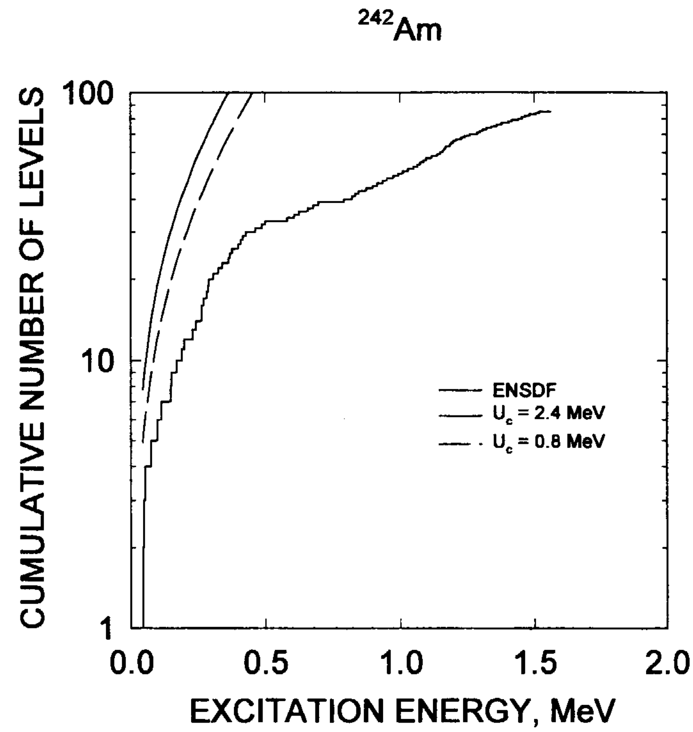

Fig. 44 Cumulative sum of low-lying levels of ^{242}Am.

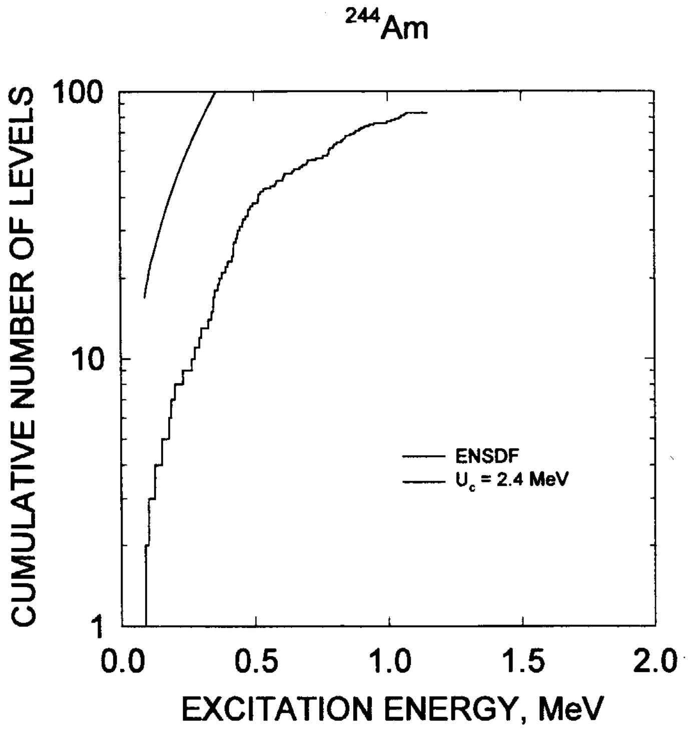

Fig. 45 Cumulative sum of low-lying levels of ^{244}Am.

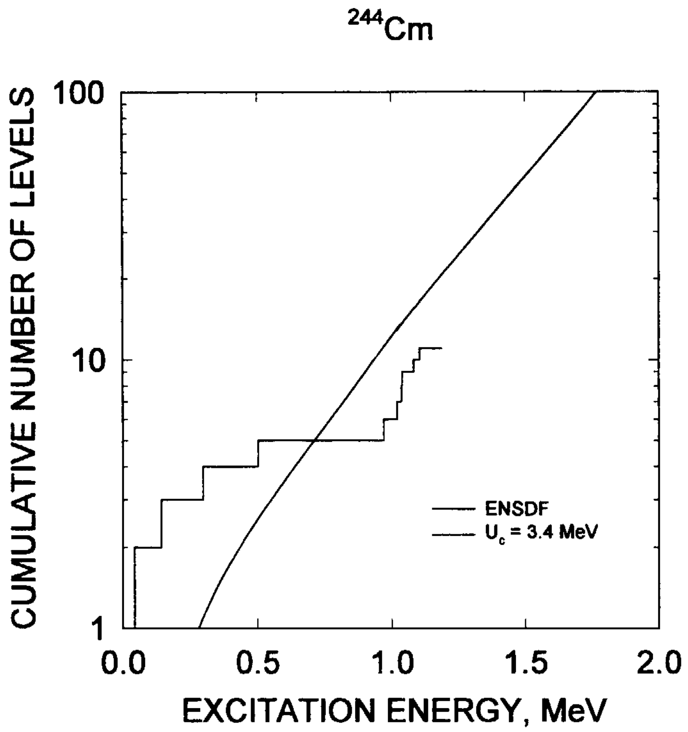

Fig. 46 Cumulative sum of low-lying levels of ^{244}Cm.

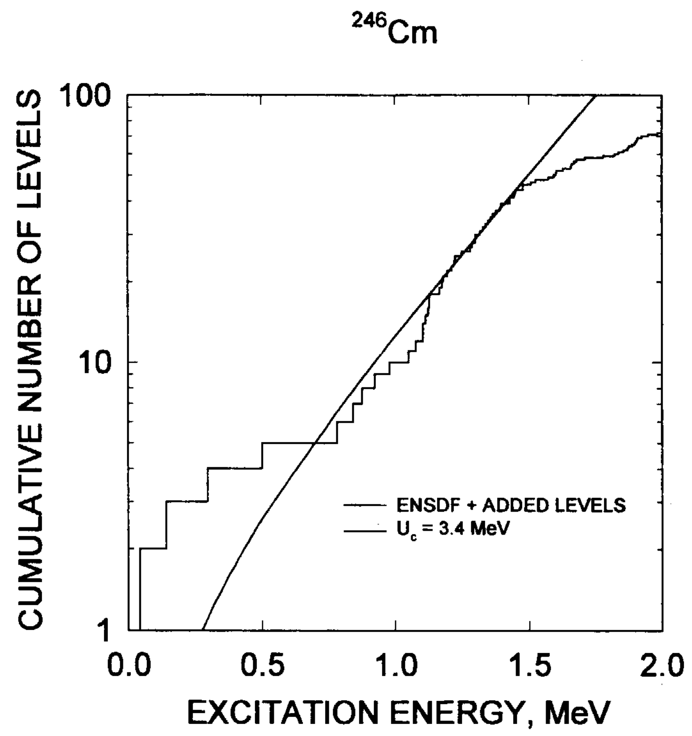

Fig. 47 Cumulative sum of low-lying levels of ^{246}Cm.

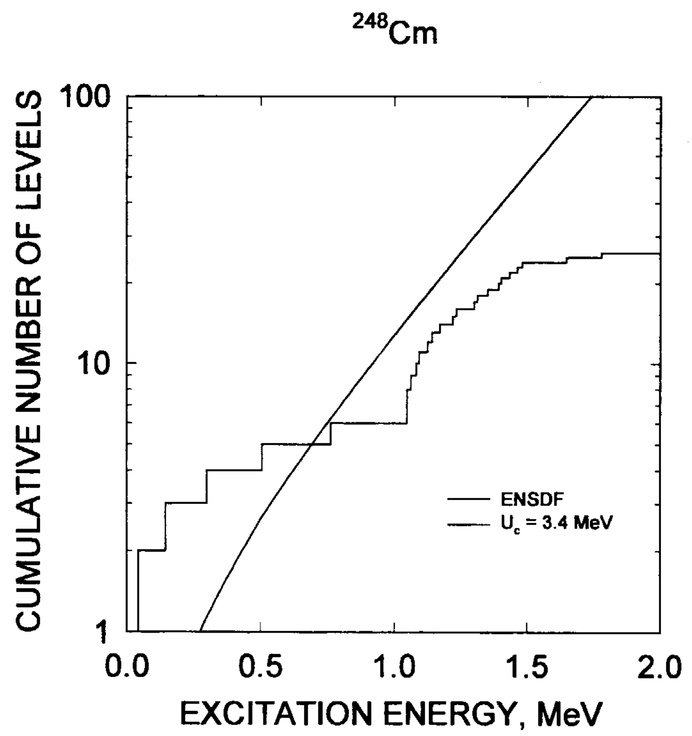

Fig. 48 Cumulative sum of low-lying levels of ^{248}Cm.

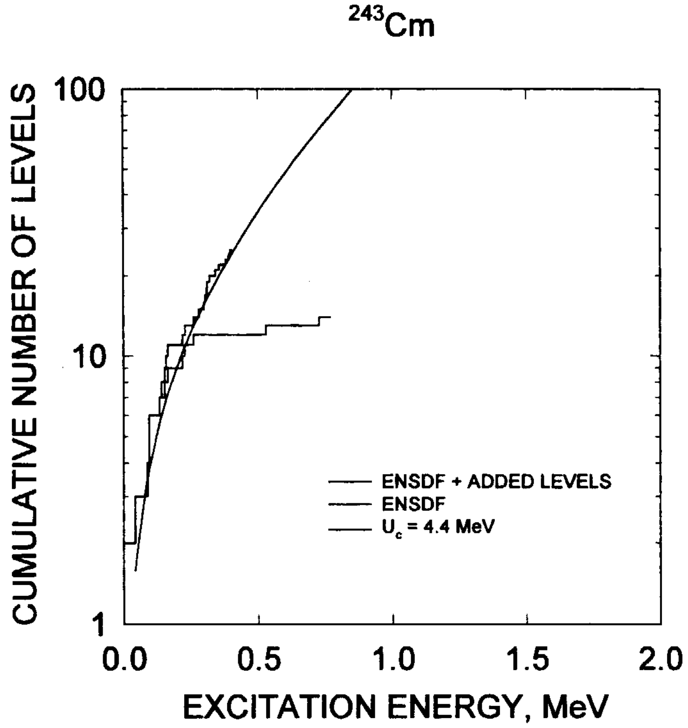

Fig. 49 Cumulative sum of low-lying levels of ^{243}Cm.

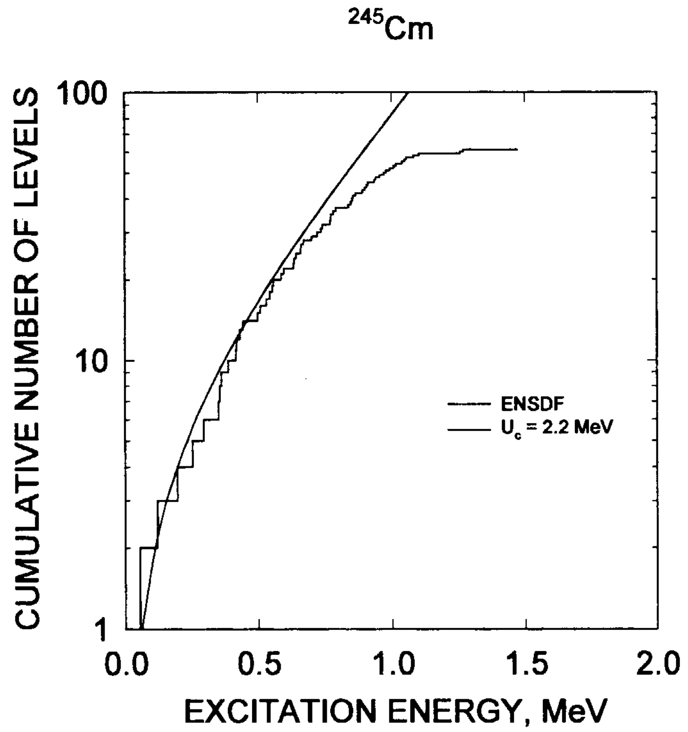

Fig. 50 Cumulative sum of low-lying levels of ^{245}Cm.

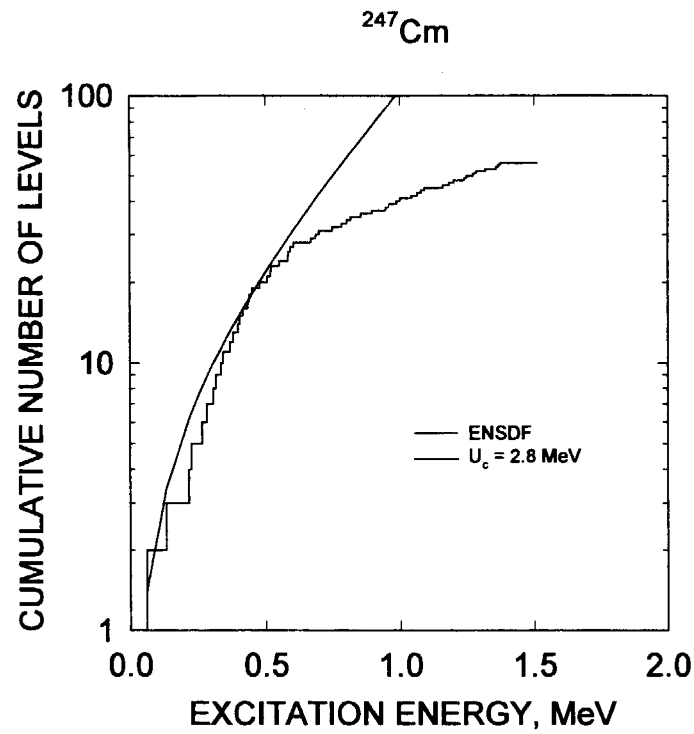

Fig. 51 Cumulative sum of low-lying levels of ^{247}Cm.

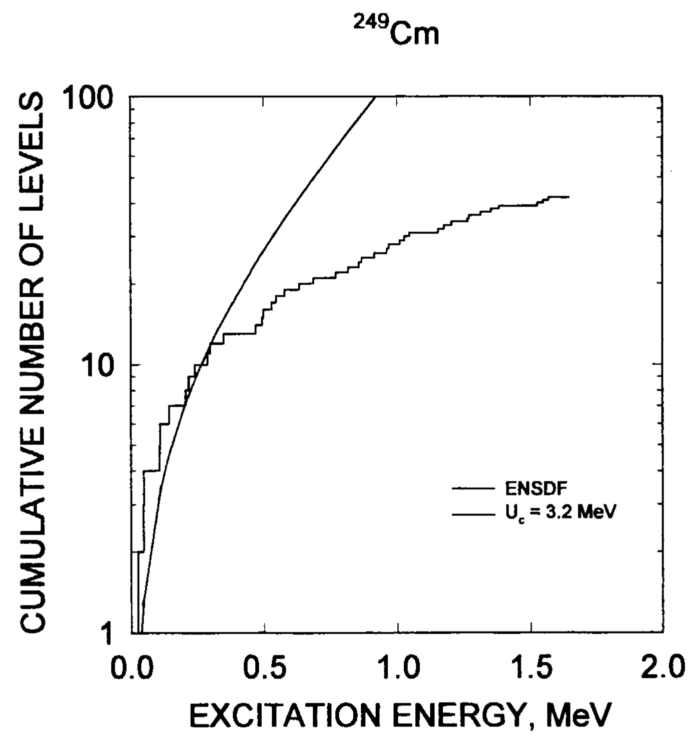

Fig. 52 Cumulative sum of low-lying levels of ^{249}Cm.

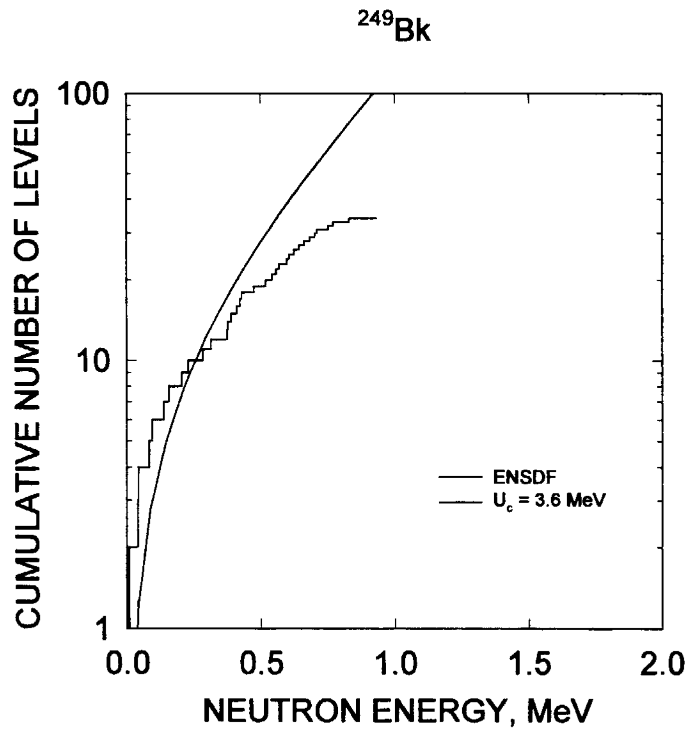

Fig. 53 Cumulative sum of low-lying levels of ^{249}Bk.

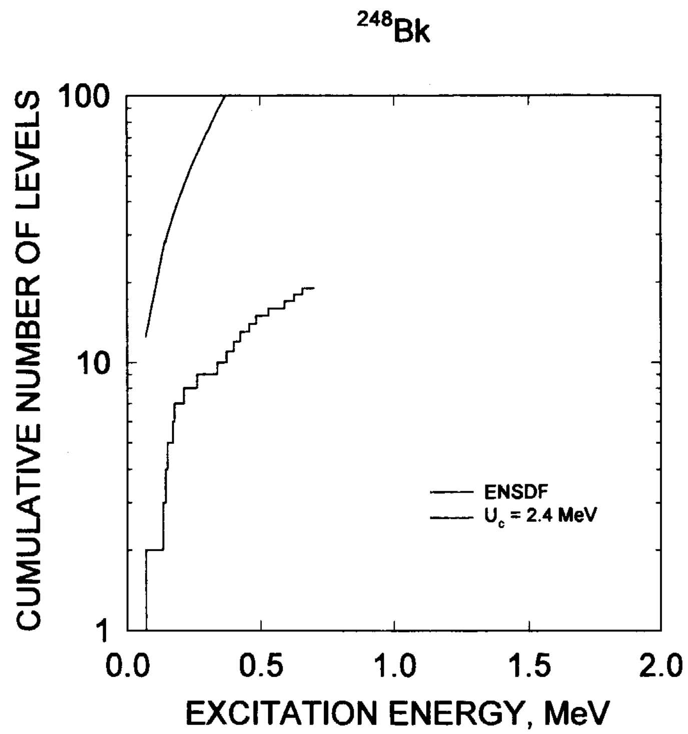

Fig. 54 Cumulative sum of low-lying levels of ^{248}Bk.

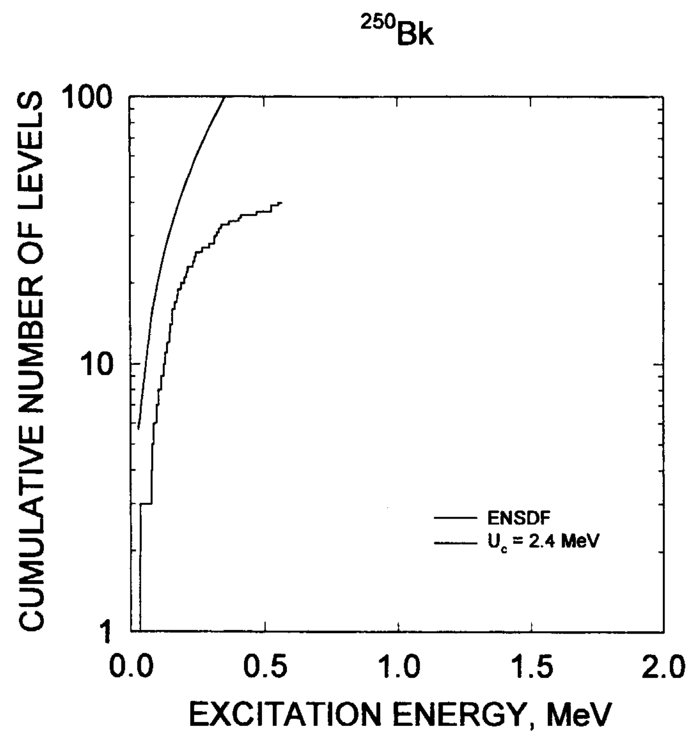

Fig. 55 Cumulative sum of low-lying levels of ^{250}Bk.

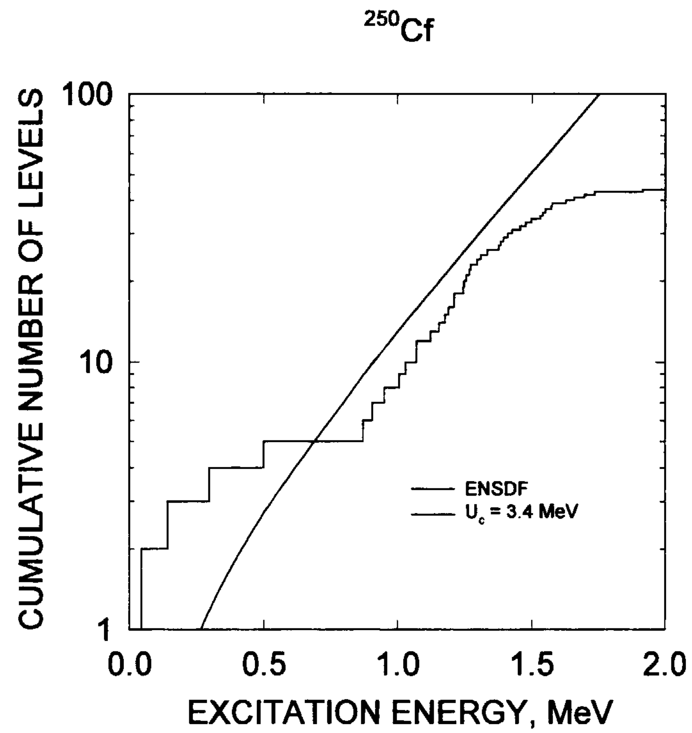

Fig. 56 Cumulative sum of low-lying levels of ^{250}Cf.

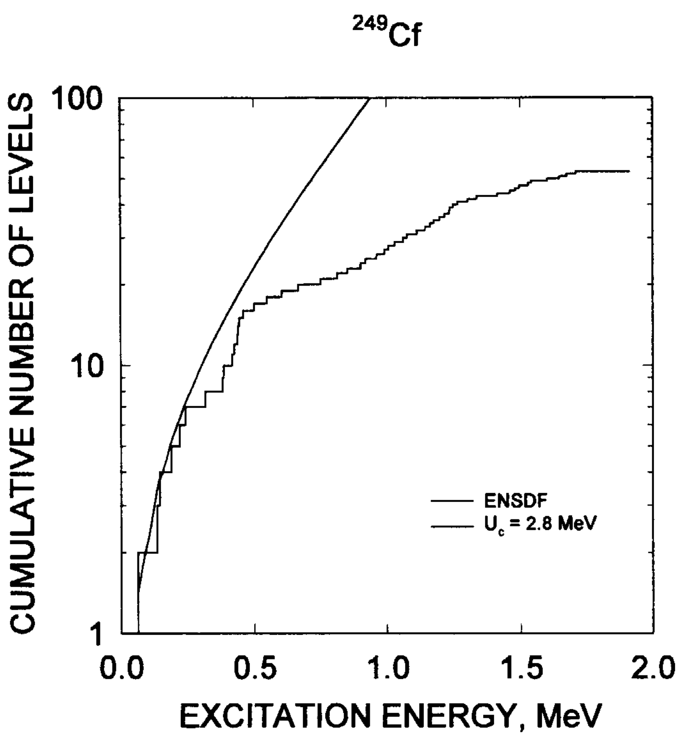

Fig. 57 Cumulative sum of low-lying levels of ^{249}Cf.

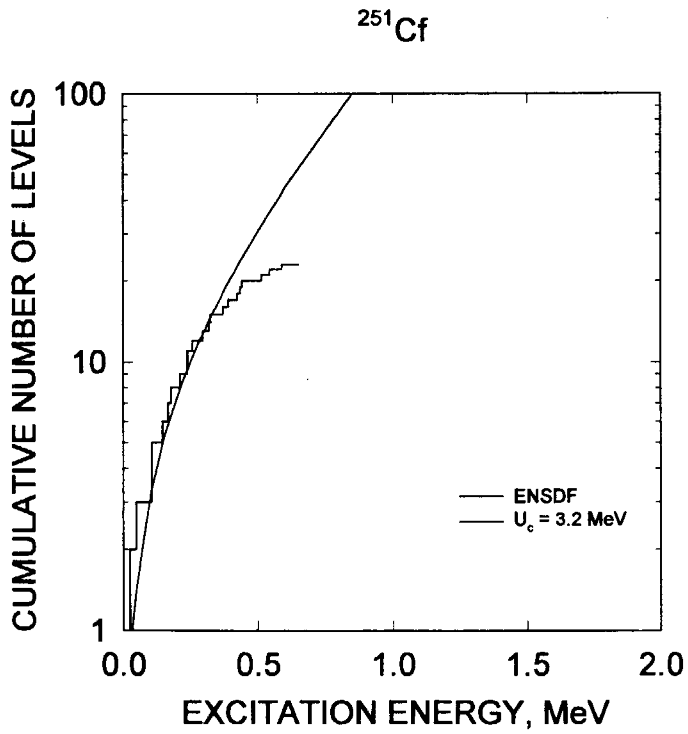

Fig. 58 Cumulative sum of low-lying levels of ^{251}Cf.

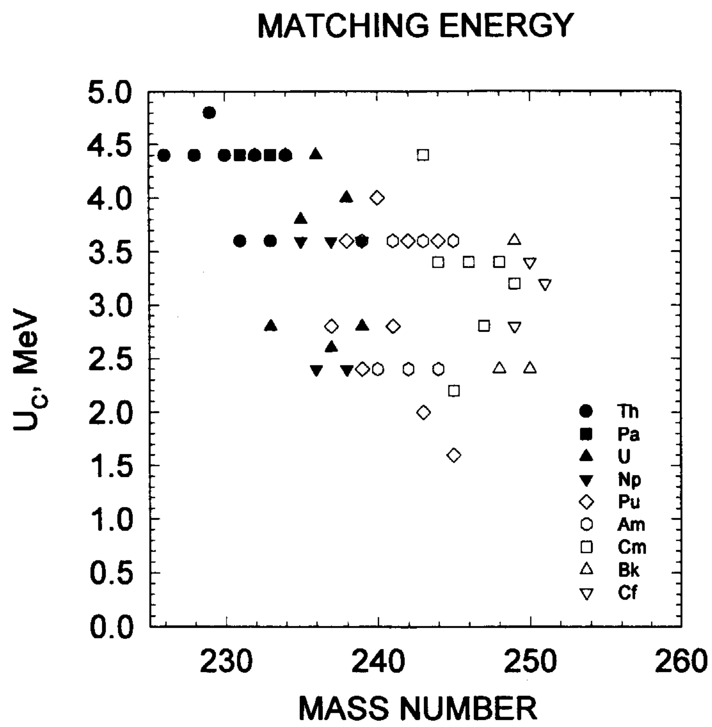

Fig. 59 Matching energy U_c.

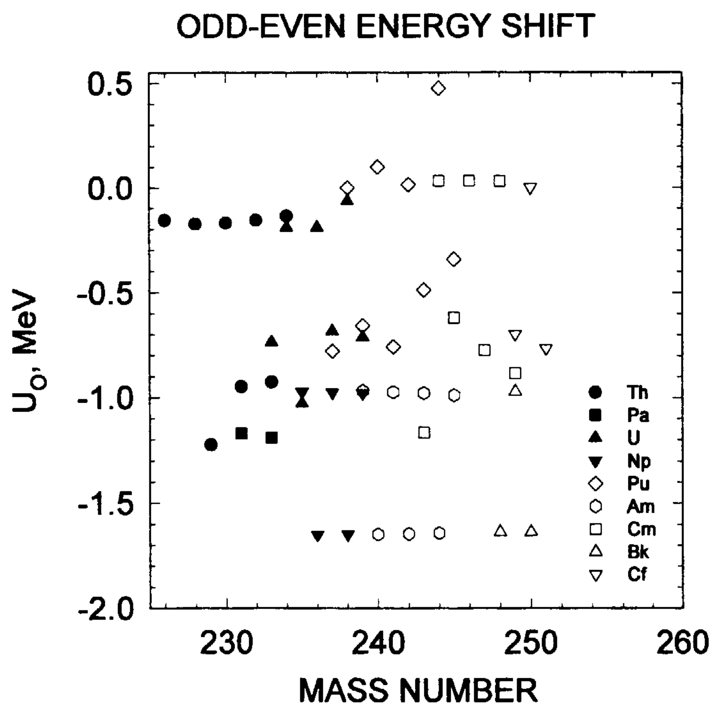

Fig. 60 Odd-even excitation energy shift U_o.

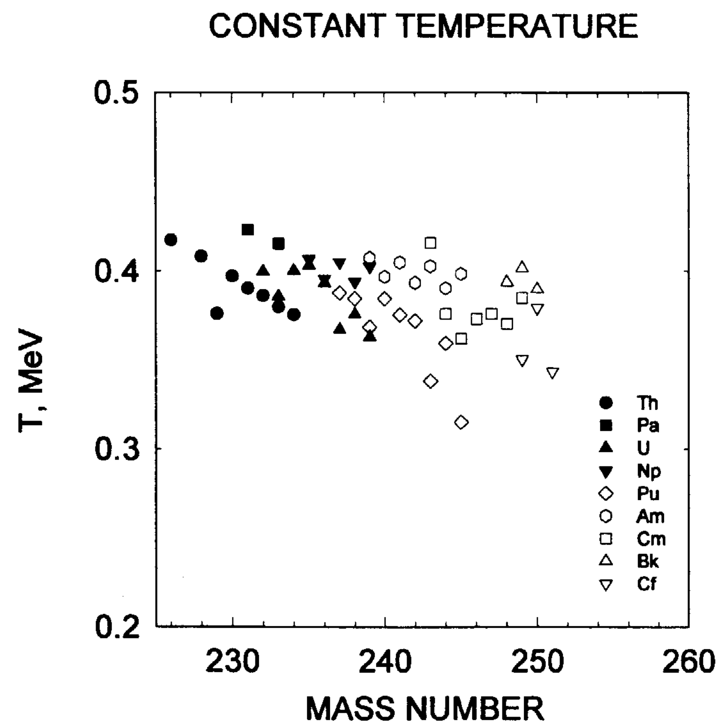

Fig. 61 Constant temperature T.

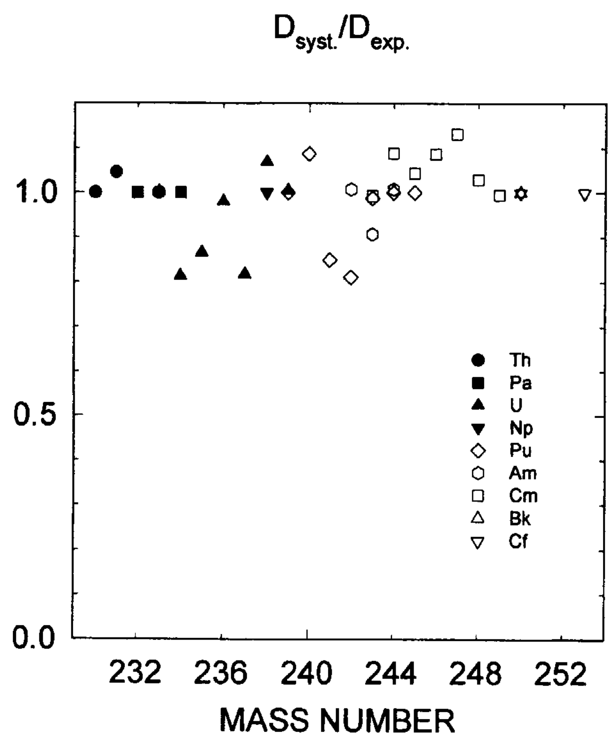

Fig. 62 Ratio of $\tilde{a}$−parameter calculated with systematic of neutron resonance spacing to the measured values.

国際単位系（SI）と換算表

表1　SI基本単位および補助単位

量	名　称	記　号
長　さ	メートル	m
質　量	キログラム	kg
時　間	秒	s
電　流	アンペア	A
熱力学温度	ケルビン	K
物質量	モル	mol
光　度	カンデラ	cd
平面角	ラジアン	rad
立体角	ステラジアン	sr

表2　SIと併用される単位

名　称	記　号
分，時，日	min, h, d
度，分，秒	°, ′, ″
リットル	l, L
トン	t
電子ボルト	eV
原子質量単位	u

1 eV=1.60218×10^{-19}J
1 u=1.66054×10^{-27}kg

表5　SI接頭語

倍数	接頭語	記　号
10^{18}	エクサ	E
10^{15}	ペタ	P
10^{12}	テラ	T
10^{9}	ギガ	G
10^{6}	メガ	M
10^{3}	キロ	k
10^{2}	ヘクト	h
10^{1}	デカ	da
10^{-1}	デシ	d
10^{-2}	センチ	c
10^{-3}	ミリ	m
10^{-6}	マイクロ	μ
10^{-9}	ナノ	n
10^{-12}	ピコ	p
10^{-15}	フェムト	f
10^{-18}	アト	a

表3　固有の名称をもつSI組立単位

量	名　称	記号	他のSI単位による表現
周波数	ヘルツ	Hz	s^{-1}
力	ニュートン	N	$m\cdot kg/s^2$
圧力，応力	パスカル	Pa	N/m^2
エネルギー,仕事,熱量	ジュール	J	N·m
工率，放射束	ワット	W	J/s
電気量，電荷	クーロン	C	A·s
電位，電圧，起電力	ボルト	V	W/A
静電容量	ファラド	F	C/V
電気抵抗	オーム	Ω	V/A
コンダクタンス	ジーメンス	S	A/V
磁束	ウェーバ	Wb	V·s
磁束密度	テスラ	T	Wb/m^2
インダクタンス	ヘンリー	H	Wb/A
セルシウス温度	セルシウス度	℃	
光束	ルーメン	lm	cd·sr
照度	ルクス	lx	lm/m^2
放射能	ベクレル	Bq	s^{-1}
吸収線量	グレイ	Gy	J/kg
線量等量	シーベルト	Sv	J/kg

表4　SIと共に暫定的に維持される単位

名　称	記　号
オングストローム	Å
バーン	b
バール	bar
ガル	Gal
キュリー	Ci
レントゲン	R
ラド	rad
レム	rem

1 Å=0.1nm=10^{-10}m
1 b=100fm^2=$10^{-28}m^2$
1 bar=0.1MPa=10^5Pa
1 Gal=1cm/s^2=$10^{-2}m/s^2$
1 Ci=3.7×10^{10}Bq
1 R=2.58×10^{-4}C/kg
1 rad=1cGy=10^{-2}Gy
1 rem=1cSv=10^{-2}Sv

(注)
1．表1−5は「国際単位系」第5版，国際度量衡局1985年刊行による。ただし，1 eVおよび1 uの値はCODATAの1986年推奨値によった。
2．表4には海里，ノット，アール，ヘクタールも含まれているが日常の単位なのでここでは省略した。
3．bar は，JISでは流体の圧力を表わす場合に限り表2のカテゴリーに分類されている。
4．EC閣僚理事会指令では bar，barnおよび「血圧の単位」mmHgを表2のカテゴリーに入れている。

換　　算　　表

力	N(=10^5dyn)	kgf	lbf
	1	0.101972	0.224809
	9.80665	1	2.20462
	4.44822	0.453592	1

粘　度　1 Pa·s($N\cdot s/m^2$)=10 P(ポアズ)(g/(cm·s))
動粘度　1m^2/s=10^4St(ストークス)(cm^2/s)

圧力	MPa(=10bar)	kgf/cm^2	atm	mmHg(Torr)	lbf/in^2(psi)
	1	10.1972	9.86923	7.50062×10^3	145.038
	0.0980665	1	0.967841	735.559	14.2233
	0.101325	1.03323	1	760	14.6959
	1.33322×10^{-4}	1.35951×10^{-3}	1.31579×10^{-3}	1	1.93368×10^{-2}
	6.89476×10^{-3}	7.03070×10^{-2}	6.80460×10^{-2}	51.7149	1

エネルギー・仕事・熱量	J(=10^7 erg)	kgf·m	kW·h	cal(計量法)	Btu	ft·lbf	eV
	1	0.101972	2.77778×10^{-7}	0.238889	9.47813×10^{-4}	0.737562	6.24150×10^{18}
	9.80665	1	2.72407×10^{-6}	2.34270	9.29487×10^{-3}	7.23301	6.12082×10^{19}
	3.6×10^6	3.67098×10^5	1	8.59999×10^5	3412.13	2.65522×10^6	2.24694×10^{25}
	4.18605	0.426858	1.16279×10^{-6}	1	3.96759×10^{-3}	3.08747	2.61272×10^{19}
	1055.06	107.586	2.93072×10^{-4}	252.042	1	778.172	6.58515×10^{21}
	1.35582	0.138255	3.76616×10^{-7}	0.323890	1.28506×10^{-3}	1	8.46233×10^{18}
	1.60218×10^{-19}	1.63377×10^{-20}	4.45050×10^{-26}	3.82743×10^{-20}	1.51857×10^{-22}	1.18171×10^{-19}	1

1 cal= 4.18605J（計量法）
= 4.184J（熱化学）
= 4.1855J（15℃）
= 4.1868J（国際蒸気表）

仕事率　1 PS(仏馬力)
= 75 kgf·m/s
= 735.499W

放射能	Bq	Ci
	1	2.70270×10^{-11}
	3.7×10^{10}	1

吸収線量	Gy	rad
	1	100
	0.01	1

照射線量	C/kg	R
	1	3876
	2.58×10^{-4}	1

線量当量	Sv	rem
	1	100
	0.01	1

（86年12月26日現在）

ACTINIDE LEVEL DENSITY PARAMETER SYSTEMATICS